MAGNETIC Fe_3O_4 NANO-STRUCTURED COATINGS FOR CORROSION PROTECTION OF MILD STEEL

by

Khalil Mohammed Abed

A Thesis Presented to the Faculty of the
American University of Sharjah
College of Engineering
in Partial Fulfillment
of the Requirements
for the Degree of

Master of Science in
Mechanical Engineering

Sharjah, United Arab Emirates

July 2014

Approval Signatures

We, the undersigned, approve the Master's Thesis of Khalil Mohammed Abed.

Thesis Title: Magnetic Fe_3O_4 Nano-Structured Coatings for Corrosion Protection of Mild Steel

Signature	**Date of Signature** (dd/mm/yyyy)
_____	_____
Dr. Taleb Ibrahim Professor, Department of Chemical Engineering Thesis Advisor	
_____	_____
Dr. Shivakumar Ranganathan Assistant Professor, Department of Mechanical Engineering Thesis Co-Advisor	
_____	_____
Dr. Bassam Abu Nabah Assistant Professor, Department of Mechanical Engineering Thesis Committee Member	
_____	_____
Dr. Nasser Qaddoumi Professor, Department of Electrical Engineering Thesis Committee Member	
_____	_____
Dr. Essam Wahba Interim Head Department of Mechanical Engineering	
_____	_____
Dr. Mohamed El-Tarhuni Associate Dean College of Engineering	
_____	_____
Dr. Leland Blank Dean College of Engineering	
_____	_____
Dr. Khaled Assaleh Director of Graduate Studies	

Acknowledgements

The fulfillment of this master's thesis has been a joint effort of a wonderful community of supporters. I am indebted to Singh, Najla, and their team at National Paints, who gave me access to their lab, helped me prepare the samples, and gave access to and assisted in conducting tests in their laboratories.

The University of Sharjah's X-Ray Center for Material Analysis was instrumental in helping me conduct analysis of the samples. I am also grateful to BYK for providing free samples that I used in my research.

I am grateful to Richard D'Souza, Technical Director at Stoncor Middle East, LLC, who provided me with free samples, technical advice, guidance, and direction throughout the research process. Dr. Nasser Hamdan connected me with valuable contacts and necessary tools. Marios Katsiosis assisted me in adjusting microscope parameters as well as giving general guidance on SEM imaging techniques.

I thank Usama Jacir, General Manager at Cortec Middle East, for his generous understanding of the demands placed on my time by my graduate work. I will always remain grateful to him for his support, advice, and mentoring throughout my studies.

Finally, I express my love and gratitude to my father and mother, and to my wife, Ruba Al Nashash, without whose care, encouragement, and patience I could not have succeeded in this endeavor. I am blessed to have you in my life.

Abstract

The use of coatings is a prime method in corrosion control of mild steel in the industry. Inorganic coatings have proven potency in corrosion control over organic ones; however, they have always been associated with a negative impact on the environment. Therefore, scientists and engineers have always been working toward improving the corrosion resistance of environmentally friendly organic coatings by different methods. This work looked into the effect of the addition of fig leaves extract, micro Fe_3O_4 pigments and Fe_3O_4 nano-particles to water-based acrylic coating in an attempt to enhance its corrosion protection properties. Both fig leaves extract and micro iron oxide powder demonstrated a corrosion-inhibitive effect when added to the coating. Upon confirming the positive impact of micro iron oxide, the effect of incorporating magnetic nano-particles Fe_3O_4 into alkyd-based enamel and water-based coatings was examined using Electrochemical Impedance Spectroscopy (EIS). For alkyd-based coating, Fe_3O_4 nano-particles were used in powder form and added during the grinding phase of preparing the coat. In addition, the effect of using glass beads during the grinding was also examined. In the case of water-based acrylic coating, Fe_3O_4 dispersion was prepared using a dispersant agent, a mechanical stirrer, and a snoicator. The dispersion was then added at the last stage of the grinding phase of the water-based acrylic coating. EIS measurements indicated an improvement on the corrosion protection properties of the alkyd-based coating. They also confirmed a positive effect for using glass beads as a grinding medium during the preparation of the alkyd-based coating. However, EIS technique exhibited a limitation in detecting the impact of incorporating Fe_3O_4 nano-particles into the water-based acrylic coating, due to the nature of its intrinsic low performance in immersion applications. Finally, an attempt was made to look inot the effect of exposing the nano-structured water-based coating to a magnetic field during the curing time of the coating. Nevertheless, It has also been difficult to infer the effect of exposing the nano-modified acrylic coating to a magnetic field due to the same reason.

Keywords: corrosion resistance, EIS, enamel coatings, fig leaves extract magnetic nano-particles, nano-Fe_3O_4, waterborne coatings.

Table of Contents

List of Figures

List of Tables

Chapter 1: Introduction

1.1 Corrosion

The yearly costs associated with corrosion inhibition and remediation have been reported to represent a substantial part of the world gross domestic product. The precise value of such costs has always been controversial. Nevertheless, corrosion undoubtedly is of great significance in our societies. Corrosion not only causes economic losses and technological disruptions, but also structural failures that can have a dramatic impact on humans and their surrounding environment. Failures in reinforced concrete structures, airplanes, automobiles, and oil and gas pipelines are only a few examples of cases in which corrosion can have detrimental effect [1].

Corrosion can be defined as the deterioration of material, usually metal, and its properties by chemical and/or electrochemical reaction with its surrounding environment[2]. For corrosion to occur, it requires an anode, cathode, an electrolytic path for the passage of ions, and an electrically conductive path for the passage of released electrons [3]. It can be stated that almost all environments in which metals are in service are theoretically corrosive, and their effective usage in engineering and commercial applications depends heavily on providing adequate protection mechanism to the subject matter metal structures [4]. Metals can be classified as passive or active, based on the nature of their reaction toward its surrounding environment. In the case of passive metals, a stable film develops naturally on the metal surface and prevents further corrosion reactions. In contrast, reactive metals react constantly with their surrounding environment and form an instable and non-protective film that allows for corrosion reactions to continue [2]. Therefore, to achieve an effective corrosion control processes, we need to fulfill one or more of the four corrosion cell requirements mentioned above. Effective corrosion control can be achieved by a single method or a combination of two or more methods, such as material selection, cathodic protection, design, inhibitors, and coatings[3].

1.2 Organic Coatings

Metals exist in the form of metallic ores in nature. They are extracted from their ores by artificial reduction reactions. Hence, metals tend to return to their original ores or to similar metallic compounds when exposed to the atmosphere. For example, iron is oxidized to ferric oxyhydroxide in a thermodynamically stable reaction. This reaction

of a metal in a natural environment is called corrosion. Therefore, corrosion is considered to be the destructive attack of a material by reaction with its environment[5].

One way to isolate structural reactive elements from the corrosive environment is through applying a layer to the metal surface to enhance its surface properties, such as appearance, adhesion, wettability, corrosion, wear, and scratch resistance. Protective coatings are undoubtedly one of the most widely implemented methods for corrosion control. They are usually classified into four main categories: organic, inorganic, conversion, and metallic. However, they all work by providing one or more of the following protection mechanisms:

1. Forming a barrier against the ingress of corrosion reactants, water, and oxygen to the metal surface
2. Creating a high electrical resistance path, thus inhibiting anode-cathode reactions
3. Passivating the metal surface with soluble inhibitive pigments
4. Providing a sacrificial anode for the dissolution process instead of the metal substrate [6]

The main protection mechanism of coatings is due to the outer shell electrons in binding media. They are mostly localized in covalent bonds; hence, coatings are poor conductors of electrons and ions. A major corrosion process cannot be established with the surrounding environment but only though the water and oxygen taken up in the coating. Coatings can be broadly divided into metallic and nonmetallic types [7]. In metallic coatings, the substrate surface is layered by a more active metal that will corrode sacrificially. On the other hand, nonmetallic coatings are either organic or inorganic. Their primary function is providing a physical barrier that isolates the substrate from its surrounding environment. Coating films are readily permeable to water and oxygen. When they are exposed to weather, they often get saturated with both. Any defectiveness in this barrier can become the focal point for degradation and corrosion of the substrate[5].

1.3 Corrosion Inhibitors

The use of corrosion inhibitors is another commonly used method of controlling corrosion of metallic components in wet environments. Corrosion inhibitors are defined as surface active solutes that, when added in small dosages to an environment, effectually reduce the corrosion rate by intervening with the corrosion kinetics. Usually,

their efficiency is proportional to their concentration: the higher the concentration, the better the corrosion inhibition efficiency[5].

Inhibitors intervene in corrosion kinetics in various ways. Inhibitor molecules that are composed of separate hydrophilic head and hydrophobic tail get adsorbed on the metal surface, forming a thin protective film[8]. They consequently reduce the corrosion rate by increasing anodic or cathodic polarization behavior, reducing the movement or diffusion of ions to the metallic surface and increasing the electrical resistance of the metallic surface[5]. Corrosion inhibitors can be classified into three main categories, as follows:

1. Passivating. These are usually inorganic oxidizing substances that suppress anodic reactions by assisting the natural passivation tendencies of metal surfaces or forming deposits that are impermeable to the metal ions, resulting in a shift in the corrosion potential in the noble direction [9-10].
2. Cathodic. These are inhibitors that either slow the cathodic reaction itself or selectively precipitate on cathodic areas to increase the surface impedance and limit the diffusion of reducible species to these areas[5].
3. Organic. Most pickling inhibitors function by forming an adsorbed layer on the metal surface, probably no more than a monolayer in thickness, which essentially blocks the discharge of H^+ and the dissolution of metal ions. This type of inhibitors requires, by and large, a favorable polar group or groups by which the molecule can attach itself to the metal surface. These include the organic N, amine, S, and OH groups. The size, orientation, shape, and electric charge of the molecule play a part in the effectiveness of inhibition [9][11-14].

With the rules and regulations getting more strict and stringent in the direction of minimizing the effect of chemical use and disposal on all aspects of life, engineers and scientists have been exploring alternative natural sources for corrosion inhibitors that will help develop environmentally friendly products.

In the last 20 years, researchers have affirmed the extraction of natural corrosion inhibitors from plant leaves, seeds, and peels [11-13]. Such natural extracts represent a potential way to create eco-friendly and cost-effective products. For example, a number of plant extracts have shown adequate protection of steel in acid mediums such as opuntia extract, aloe eru leaves, orange and mango peels, tobacco, black pepper, castor oil seeds, acacia gum and lignin, onion, garlic, and bitter gourd[10].

1.4 Nanotechnology

Nanotechnology is considered to be one of the strategic technologies for the future of human beings. The term "nanotechnology" is referred to as the manufacturing, analysis, and use of structures, for example particles, layers, or tubes of less than 100 nanometers (nm) in at least one dimension [11]. Nano-sized particles and nanoscale system components exhibit new properties and characteristics which are of importance to the development of new products and applications. One of the applications that has created considerable interest is the incorporation of nano-particles into polymers for a variety of applications, including organic coatings. This seems to be a logical development from the conventional technique of improving properties of polymers by the addition of micro-sized particles and fibers. However, researchers have found that the addition of nano-sized particles can have a positive impact on corrosion resistance and the mechanical properties of organic coatings at comparatively low loadings[12].

1.5 Electrochemical Impedance Spectroscopy (EIS)

The electrochemical nature of the corrosion process lends itself to the use of electrochemical corrosion testing methods, which are extremely useful for the determination of the corrosion behavior of alloys and coatings in corrosive environments. Most forms of corrosion can be investigated with electrochemical techniques and provide quick, accurate, and dependable data that can be used in corrosion investigations, the selection of materials for corrosive environments, and prevention of corrosion failure [17-18]. Electrochemical Impedance Spectroscopy (EIS) is a non-destructive research technique that can obtain vital information about interfacial material parameters through the use of low-energy, time-varying electrical excitation. EIS can give insight into corrosion rates, coating porosity, integrity, and mass transport through it, and many other characteristics at the interface between the coat and the substrate [19-20].

1.6 Thesis Objective and Contribution

The deployment of nanotechnology in improving the corrosion protection properties of organic coatings has lately gained impetus due to the unique physical, chemical, mechanical, optical and magnetic properties of nanoscale materials compared to bulk-size materials. Substantial work on nano-structured coatings is ongoing worldwide. For example, there are studies that focus on investigating methods of incorporating and dispersing compatible nano-particles into organic coatings[13]. On

the other hand, there are studies that examine the impact of shape, size, and surface treatment of nano-particles on the final coating's properties[14]. Nanotechnology has positive potential not only for economic development, but also with regard to the protection of existing infrastructure and human health. Nanotechnology development may help protect mild steel structures by enhancing the overall performance of corrosion protection properties of organic coatings.

The objective of this work is to take part in this contemporary worldwide research topic and contribute to its momentum through enhancing the corrosion protection properties of conventional Zinc Phosphate alkyd-based enamel and water-based coatings by incorporating magnetic Fe_3O_4 nano-particles into the coatings during the grinding phase and distributing them throughout the coating matrix using a magnetic field during the curing phase. This novel approach of using a magnetic field aims to affect the distribution of the nano-particles in the coating's matrix. This in turn is believed to create a better barrier effect and reduce the transport paths of corrosive species through the coating thickness.

1.7 Thesis Organization

This thesis is organized into five chapters. Chapter Two is the literature review, in which critical points and fundamental findings related to the use of nano materials in organic coatings and the most commonly used experimental procedures are highlighted.

Chapter Three discusses the materials and experimental procedures that were utilized throughout the development of this thesis, such as raw materials, panel preparations, coating applications, characterizations, corrosion tests, and, finally, imaging techniques.

Chapter Four presents analyses and depicts the results and findings of the different tests and characterization techniques from Chapter Three.

Chapter Five concludes the thesis, summarizes its main results, and presents possible future research avenues.

Chapter 2: Literature Review

2.1 Organic Coatings

2.1.1 Composition.

Steel has always been an essential part of all industries for several engineering and economic reasons. However, it requires constant protection against corrosion during its service life to avoid catastrophic accidents and conserve our natural resources[15]. Metallic and nonmetallic coatings, corrosion inhibitors, and cathodic protection are methods that have been applied intensively to protect mild steel structures. However, anticorrosive organic coatings have always been the most widely used protection technology.

The composition of anticorrosive organic coatings is a complex formulation made of several chemicals and materials, each of which serves a single or multiple functions. Nevertheless, coatings normally consist of four basic components: solvents, binders, pigments, and additives[16]. When a coating is applied, the solvent evaporates during the curing process, leaving only the resin and the pigment components, which form the protective film on the substrate.

Organic solvents are formulated into coatings to dissolve the resin component, control evaporation for film formation, and reduce the coating viscosity for ease of application. Solvents will also affect dry film adhesion and durability [17]. Besides the compatibility requirement of the solvent with the binder used, the solvent evaporation rate can have a major impact on the properties of the coating, and several common visible and invisible defects can be traced to an inappropriate choice of solvents[16]. As the solvent evaporates during curing, volatile organic components escape into the air and react with air pollutants under the influence of UV from sunlight to form smog that depletes the ozone layer.

Binders are the film-forming component of a coating and provide the physical structure to bind itself to the pigments and additives and to the substrate. They are mostly organic, consisting of natural resins or man-made polymers or pre-polymers, such as acrylics, alkyds, vinyls, natural resins and oils, epoxies, and urethanes[16]. Many of the coating’s physical and mechanical properties - including flexibility, hardness, chemical resistances, UV-vulnerability, and water and oxygen transport - are determined wholly or in part by the particular polymer or combination of polymers used

[6]. Because no single binder type can satisfy the previously mentioned properties, a blend of monomers and polymers are used in coating formulations.

Pigments are either organic or inorganic and they directly impact different coating properties such as color, opacity, moisture and fungus resistance, corrosion resistance, and slip resistance. Inorganic pigments are crystalline solid particles. They are dispersed in the binders through the use of special additives such as dispersants. Additives are usually added in minute amounts to help homogenize the widely varying molecular weights, physical properties, and chemical properties of the different components and confer specific properties to the coating, such as anti-settling agents, viscosity modifiers, defoamers, driers, surfactants and corrosion inhibitors [23-24].

It is very important to note that anticorrosive organic coatings are complex systems wherein a wide variety of both inorganic and organic materials of widely varying molecular weight and physical properties are combined together and expected to act as a homogeneous whole. This is due to the fact that coatings are exposed to different environments, such as constant immersion in water, exposure to splash zones, or atmospheric exposure to pollutants in industrial areas. Therefore, the design and selection of anticorrosive coatings are highly dependent on the environment to which the coating will be exposed to during its service life [1].

2.1.2 Protection mechanisms.

Anticorrosive coatings are usually categorized according to the mechanisms by which they protect a metal against corrosion. They can create an effective barrier against the corrosive elements, water and oxygen; create a path of extremely high electrical resistance inhibiting anode-cathode reactions; or provide corrosion inhibitor soluble pigments or an alternative anode for the dissolution process. Therefore, they are either barrier coatings, inhibitive coatings or sacrificial coatings.

Barrier protection is achieved by applying a coating system that has low permeability for ions, liquids, and gases. Such low permeability hinders the transport of aggressive species into the surface of the substrate and therefore isolates it from its environment. Studies have shown that effective barrier protection depends on the ionic impenetrability of the coatings, which ensures that moisture at the interface between the substrate and the coating has very low ions or, alternatively, high electrical resistance. Thus, the conductivity of the electrolyte solution at the substrate is so low that the transfer of corrosion current between the anode and cathode is minimized[1].

Barrier coatings use an inert pigment, such as titanium dioxide, micaceous iron oxide, or glass flakes, at lower pigment volume concentrations. This lower pigment volume concentration yields to dense and cohesive coatings that exhibit very low permeability towards corrosive elements or species. The level of protection offered by a barrier coating system depends on the thickness of the coating system and orientation and shape of pigments[11].

Inhibitive protection is achieved by the addition of inhibitive pigments to the coating. The inhibitive pigments passivate the substrate and build a defensive film consisting of insoluble metallic complexes, which in turn hinders corrosion. The inhibitive pigments are inorganic salts that are marginally soluble in water. When the coating is permeated by water, the pigments partially dissolve and are carried to the substrate surface. At the surface of the substrate, the dissolved ions react with the substrate and form a reaction product that passivates the surface of substrate[16] [18]. Due to the slow and partial solubility of organic salts in diffusing moisture, enough inhibitive pigments should be incorporated in the coating to ensure the sufficient leaching of pigments from the coating. Conversely, if the solubility of the inhibitive pigments is too high, blistering may take place [19].

The sacrificial mechanism relies on the concept of galvanic corrosion by which the coating includes pigments that are electrochemically more active than the substrate to be protected. The inhibitive pigment, such as zinc, will behave like an anode and sacrifice itself to protect the metal, which will be the cathode through the transfer of galvanic current [20]. This working mechanism calls for continuous direct contact between the pigment and the substrate. Hence, very high loadings of inhibitive pigment are required, which come at the expense of the other components' percentages in the formulation of the coating, such as binders. This in turn has a direct negative impact on the mechanical properties, impact resistance, adhesive, and cohesive strengths of the coating[6].

It must be noted that it is impossible to use all these mechanisms in one coating. However, all coatings suffer from one of or a combination of the rate-controlling factors discussed hereafter.

1.1.2.1 Diffusion of water and oxygen.

The majority of coatings do not protect metal substrates by preventing the diffusion of water and oxygen. Studies have shown that the amount of moisture that

can diffuse through organic coatings is far more than what is required to sustain the cathode reaction and hence corrosion process[21]. For example, the amount of water necessary for corrosion to occur at a rate of 0.07 g Fe/cm^2/year is approximately 0.93 g/m^2/day. Therefore, a sufficient thickness of very low permeability rates can be used to stop moisture from reaching the metal surface in quantities necessary to start and sustain the corrosion process. Other protection mechanisms should be applied for coatings with high permeability rates[6] [21]. Nevertheless, the effect of water diffusion through the coating cannot be completely disregarded. Studies have pointed out that, even though water permeability is not normally the rate-controlling factor in the corrosion of coated substrate, it may be the rate-determining factor in loss of adhesion[22].

In the case of oxygen, the threshold amount of oxygen required to sustain the same corrosion rate of 0.07 g Fe/cm²/year is 575 cc/m²/day, which is far less than what is needed to maintain a corrosion reaction at the metal interface. Properly formulated coatings are able to eliminate sufficient oxygen from the metal surface and impede the cathodic reaction and therefore corrosion process. Generally, water and oxygen are essential for the corrosion process; however, their permeation through the coating is not a rate-determining factor[6] [21].

1.1.2.2 Ionic resistance.

The main protection function of organic coatings is to create paths of extremely high electrical resistance between cathode and anode areas and hinder the flow of current between those sites. This is accomplished by blocking the transport of ions through coating thickness and hence preventing the formation of soluble ferrous compounds. As mentioned earlier, most coatings allow the diffusion of water, but not ions. Therefore, the water that reaches the substrate surface is almost ion-free. This is not conducive to the corrosion process, as steel corrodes very slowly in pure water. This is due to the fact that ferrous ions and hydroxyl ions form $Fe(OH_2)$ compounds of low solubility in water (0.0067 g/L at 20°C). Such compounds precipitate at the corrosion sites and prevent further diffusion[6]. In the presence of corrosive anions such as Cl^-or SO^{-2}, they will react with steel and form soluble chemical compounds that can be hydrolyzed, oxidized, and precipitated away from the corrosion site. Studies have shown that there is a direct relationship between the corrosion protection of the coating and its ionic resistance value. One study showed that coatings that could sustain an

ionic resistance of 108 Ω/cm² after an exposure of several months demonstrated good corrosion protection, compared to coatings which exhibited lower ionic resistance values[23]. It has also been shown that ionic resistance of immersed coatings could change over time through two different processes. The first process takes place immediately after the immersion and is attributed to the amount of water in the coating film. This fast process is controlled by osmotic pressure. The second process, on the other hand, is a slow one, and is controlled by the concentration of electrolytes in the solution. It is believed that the slow exchange of cations in the electrolyte for hydrogen ions in the coating is responsible for the long-term and constant decrease in the ionic resistance and the physical deterioration of the coating [32-35].

1.1.2.3 Adhesion.

The capacity of the bond to keep strong contact between the coating and the substrate surface at the atomic level plays a vital role in the protection capability of the coating. Very strong adhesion suppresses hydrogen evolution and water build-up at the coating/substrate interface. It also prevents the development of corrosion products by bonding to the cathode and anode area and works as an insulator between those sides [36-37]. Wet adhesion is considered to be more decisive in corrosion than dry adhesion[6]. Coatings tend to become saturated with water, or water vapor, and their ability to still adhere to the substrate surface controls the anticorrosive properties of the coatings. It is very important to differentiate between the initial adhesion values and the capacity of the coating to retain such adhesion values after weathering. Therefore, it is very important to conduct adhesion tests not only on the freshly coated samples, but also on stressed coated samples. [24].

2.1.3 Environmental compliance.

The stringent international and national volatile organic compounds (VOC) legislation has led to significant changes in the formulation of anticorrosive coatings. Restrictions on the VOC content of coatings have been decreed by many air pollution control districts. Such legislation prohibits the manufacture, sale, or use of industrial maintenance primers and topcoats if the VOC level exceeds certain limits, commonly 420 g/L or 350 g/L[15] [25]. It has been determined that almost all volatile solvents react under the influence of UV light and degrade to form smog that helps deplete the ozone layer [1].

The current quest to reduce VOC content in coatings has urged and will continue to urge the manufacturers and developers of coatings to formulate coatings with high solid contents, powder coatings, or waterborne coatings with as low amounts of organic solvents as possible. Although high-solid, inorganic, waterborne, and powder coatings are becoming more often applied, it may be difficult to completely replace solvent-borne organic coatings in very corrosive environments.

2.2 Natural Corrosion Inhibitors

The use of corrosion inhibitors is one of the most common methods of corrosion control and mitigation. These inhibitors are defined as chemical substances that, when added in minute amounts to a corrosive environment inhibit or reduce the rate of corrosion of the metal with its surrounding media. This is usually achieved by altering the kinetics of anodic and/or cathodic reactions, lessening the rate of diffusion of corrosive elements to the metal surface and decreasing its electrical resistance[10].

Many synthetic heterocyclic compounds containing O, N, S, and P have shown good corrosion inhibition abilities due to their high levels of basicity and electron density. The majority of these compounds, when added to media surrounding the metal object, get adsorbed onto the metal surface and create a protective layer of one or several molecules thick. The formation of this barrier is facilitated by the transfer of a free pair of electrons from the corrosion inhibitor to the metal surface. However, the stability of the formed barrier depends on the electron density of the donor atom and the polarizability of the functional group. Although synthetic corrosion inhibitors have demonstrated good performance, they have generally been associated with a high level of toxicity for humans and the environment [26].

Natural corrosion inhibitors are usually produced from plant extracts such as dried seeds, peels, leaves, or stems. Studies have also shown that they can be produced from byproducts of food, meat, and milk industries. Attributable to their availability, bio-based nature, biodegradability, and cost effectiveness, green inhibitors have become recognized as a viable potential alternative for expensive and toxic organic inhibitors. In recent decades, significant efforts have been dedicated to find effective natural corrosion inhibitors in different corrosive media. As a result, several research works have reported naturally occurring substances such as plant extracts to inhibit the corrosion of mild steel in acidic, neutral, and alkaline environments.

Saleh, et al. found that extracts of opuntia, aleo eru leaves, orange and mango peels, Hibiscus subdariffa, and beet root can provide satisfactory corrosion protection to steel in different concentrations of HCl solutions and at different temperatures [41-43]. Zucchi, et al. confirmed that plant extracts of papaya, poinciana pulcherrima, cassia occidentalis, datura stramonium seeds, calotropis procera, and azadirachta indica reduced steel corrosion with an efficiency of up to 96% in 1 N HCl solution[27]. The use of coriander, anis, black cumin, hibiscus, and garden cress as new types of natural inhibitors of the acidic corrosion of steel was suggested by Khamis, et al. [28]. El-Etre, et al. proposed the use of natural honey as corrosion inhibitor for carbon steel in aqueous solution, and examined khillah extract and lawsonia extract for the corrosion inhibition of different steels in acid solution [46-48]. Mehta, et al. have studied the anticorrosion properties of embilica officianilis, Terminalia chebula, Terminalia belivia , Sapindus trifolianus, accacia conicianna, trifla, extracts of Swertia angustifolia, and eugenia jambolans [49-52]. Many other scientists have looked into other plant extracts and oils as green corrosion inhibitors, such as Eucalyptus leaves, pongamia glabra, Annona squamosa , Azadirachta indica, Carica papaya, amydalina, henna, bgugaine, ginger , artemisia oil, and jojoba oil in acid solutions. Others have examined the efficiency of Telforia occidentalis extract, Berberine (an alkaloid isolated from Captis) in the corrosion inhibition of mild steel in H_2SO_4 media [53-64].

Ibrahim, et al. examined the corrosion inhibition capabilities of fig leaves extract, eggplant peel extract, potato peel extract, and thyme leaves extract of mild steel in different concentrations of hydrochloric acid solutions and at different temperatures using conventional weight loss measurements and several electrochemical techniques, such as Tafel polarization, linear polarization, cyclic sweep, and electrochemical impedance spectroscopy. It has been proved that the addition of the different extracts to the corrosive media showed an increase in the charge transfer resistance and a decrease in the value of the double layer capacitance, indicating the adsorption of inhibiting molecules onto the metal surface following Langmuir adsorption isotherm at all test temperatures. The Tafel slopes revealed that these extracts work as mixed-type inhibitors, wherein they lower both cathodic and anodic currents. The linear polarization measurements showed inhibition efficiencies ranging between 75% and 90% at 400 ppm and at 25°C [8][65-67].

2.3 Nano Materials

As mentioned earlier, pigments form a crucial element of many organic coating formulations. They usually consist of micro-sized particles that are dispersed in the coating binder to endow both aesthetic and protective properties to the coating. A number of limitations and coating defects have been reported for conventional micro-sized pigments[4] [12]. Problems such as poor adhesion and early delamination, and inferior scratch and abrasion resistance, are examples of various drawbacks associated with the use of conventional pigments[3].

Diffusion of water through the coating and disbondment propagation between the coating and the substrate are the two main mechanisms for the breakdown of coating protection. One recent technique that has been used to increase the adhesive and anti-corrosive properties of organic coatings is the incorporation of nano-particles into the coating system[29]. Nano-sized fillers can provide superior barrier properties to conventional fillers even at low concentrations due to their large surface area to volume ratio [2].

The most commonly used nano-particles in coatings are SiO_2, TiO_2, ZnO, Al_2O_3, Fe_2O_3, $CaCO_3$, single-wall carbon nano-tubes (SWCNT), and multi-walled carbon nano-tubes (MWCNT. A combination of two different nano-particles has been used to achieve the required results, TiO_2 with Al_2O_3; and CeO_2 and Cr_2O_3. The average size of nano-particles usually ranges from 5 nm to 100 nm [2] [4] [12][68-73].

The proper incorporation of nano-particles into the coating matrix is critical for achieving the desired properties in the formulated coating. Both the method and stage of introducing the nano-particles are critical. Shi, et al. introduced the nano-particles with the solvent and added the curing agent to the mixture[30]. Gao, et al. added the $CaCO_3$ in the form of a dispersion into the polypropylene and left it to dry at 60 °C[31]. Dhoke , et al. dispersed Fe_2O_3 and ZnO nano-particles into the alkyd-based waterborne coating using mechanical stirring followed by ultra-sonication [3] [32]. While, Lewis, et al. used a ball-milling technique to disperse uncoated rutile titanium dioxide waterborne acrylic coating [12]. The percentage loading of nano-particles is another critical factor that plays a key role in developing the successful formulation of any nano composite coating. Loading percentages ranged from.01 to 10% wt. [2-4] [32].

The improvement in the corrosion resistance of the nano-structured coating systems could be attributed to the large surface area to volume ratio of the nano-particles. This high ratio allows for more resin to get adsorbed on the particle's surface

and hence reduces the transport paths for the corrosive electrolyte to pass through the coating system[32]. It is also believed that this high ratio not only increases the likelihood of diffusing moisture and ions to interact with the particles, but also increases the possibility of adsorbing the moisture onto the particles' surface[12]. The improvement can also be attributed to diminishing the interspaces and hence improving the density of the coatings [33]. Enhancement of the mechanical properties of the coating systems, such as scratch and abrasion resistance, might be due to the strong surface interaction between the dispersed nano-particles and polymer matrix, which provides strength to the system and does not allow the coating to detach from the substrate [3]. Another positive effect on the mechanical properties is the tensile strength of the coating, which is attributed to the increase in the cohesiveness of the coating, which also might have a direct impact on the corrosion resistance[29].

One class of nano-particles has drawn the attention of scientists and engineers in a wide range of disciplines such as biotechnology, magnetic fluids catalysis, and environment remediation: magnetic nano-particles. This is due to their outstanding magnetic properties and the energy originating from the high surface area to volume ratio. Moreover, bare nano magnetic particles usually have a very high level of surface chemical activity, which results in high oxidation rates when exposed to air and other media, such as water. One way to overcome this challenge is to coat the core with hydrophilic polymers, such as coating $Fe3O_4$ nano magnetic particles with starch. [76-77]

2.4 Electrochemical Impedance Spectroscopy

It is well known that EIS is a powerful tool that is now being broadly utilized in a wide range of scientific disciplines such as fuel cell testing, biomolecular interaction, and microstructural characterization and corrosion studies. EIS technique has grown tremendously in importance over the last couple of decades in the field of corrosion testing due to its accurate and reliable corrosion rate measurements[5]. It has also proven to be a very helpful tool in the evaluation and prediction of coatings' protective quality on metal substrates by detecting the changes in coating barrier qualities [1-2] [4][6-7] [20][69-72]. EIS is a non-destructive technique that gives researchers an opportunity to provide quantitative data for a coated metal immersed in an electrolytic solution that can be related to the performance of the coating in corrosion protection of the metal substrate at an early stage before any visual damage takes place.

Tests designed to evaluate coatings always involve the use of a mechanism to stress the coating and accelerate deterioration in a simulated environment that is believed to bear a resemblance to the intended application. EIS measurements at a predefined pattern during that process can be utilized to track the changes in the coatings' integrity and determine the corrosion rate of that metal substrate. For example, it can measure the change in coating capacitance and its porosity[34].

EIS, also known as AC impedance, involves the use of AC voltage excitation over a wide range of frequencies, 1×10^{-4} Hz to 100 kHz. This range helps the EIS to offer rich information about the coating system and its behavior. It also requires the use of a physic-electrical model or an equivalent circuit to quantify the physiochemical changes taking place in the system[35]. The electrical circuit models are built from components such as resistors, capacitors, and other non-standard circuit elements, like double layer capacitance element, to simulate the electrochemical behavior of the system by tracking the changes in the values of the different elements during the test period[1].

Aglan, et al. used the basic Randle electrochemical cell model and a frequency range from 1×10^{-2} Hz to $1x10^{6}$ Hz with amplitude of 10 mv and an immersion period varied up to 70 days without using any stressing mechanism [29]. Lewis, et al. used the neutral salt spray corrosion testing and backed it up with EIS tests from 100 mHz to 50 kHz with 10 mv amplitude and 10 points per decade. The tests were conducted after 24 hours, 48 hours, 168 hours, and 336 hours[12]. Dhoke, et al. acquired EIS spectra over a frequency range of 1 Hz to 100 kHz and 5 mV amplitude and software was used to fit the results into an equivalent circuit[4]. Behzadnasab, et al. took eight EIS measurements during 120 days at an open circuit potential with a frequency range of 1×10^{-4} Hz to 10 kHz [2] . While, Kartsonakis, et al. used a frequency range from 5 mHz to 100 kHz with rms voltage of 10 mV and the spectra were collected after 1 hour, 20 hours, 46 hours, 68 hours, 4 days, 6 days, 8 days, and 28 days, and treated using software to fit the data and come up with the best fit [36].

Chapter 3: Materials & Experimental Procedure

3.1 Raw Materials, Equipment, and Software

Materials included in-house-made fig leaves extract with an average of 14,000 ppm concentration; high purity Fe_3O_4 nano-powder with an average size of 15-20 nm, specific area of (BET) = 81.98 m^2/g and true density of 4.8-5.1g/cm3 purchased from US Research Nanomaterials, Inc.

DISPERBYK-2015; VOC-free wetting and dispersing additive for waterborne systems and BYK-D 420; liquid rheology additive water-reducible systems and pigment concentrates were sourced from BYK-GARDNER GMBH.

Zinc phosphate alkyd-based enamel coating was sourced from National Paints Factories Co. Ltd. While, Zinc phosphate water based acrylic coating was developed and formulated by Unichem Group, Jordan.

Mild steel panels Mild steel panels with a composition of (0.037 C; 0.0090 P, 0.0140 S; 0.151Mn; 0.001Si; 0.026 Sa; 0.0028 N, 0,017 Cr, 0.001 Mo, 0.028 Ni, 0.028 Al, 0.0020As, 0.0029 Bo, 0.001 Co, 0.019 Cu, 0.001 Nb, 0.004 Sn, 0.001 Ti, 0.001 V, 0.0002 Ca, 0.069 CEV, and balance is Fe) were procured from PRO TEST PANELS LTD.

Q500 Sonicator was purchased from Qsonica, LLC and used in the preparation of the aqueous dispersion of Fe_3O_4 nano-powder. Gill AC potentiotstat and cathodic disbondment test cells from ACM instruments were used for AC impedance and cathodic disbondment tests along with a Faraday cage that was fabricated in AUS engineering workshop. Different types of mechanical stirrers for production of the different coatings were used at National Paints Factories Co. Ltd.

ZView® software from SCRIBNER ASSOCIATES INC and Sequencer from ACM were utilized for modeling and analysis of acquired IES spectra.

3.2 Coating and Panel Preparation

The first phase of this research was to understand the effect of incorporating micro Fe_3O_4 pigments on the corrosion protection abilities of the coating to validate the feasibility of moving to the nano size iron oxide. Therefore, Zinc Phosphate water-based coating was outsourced with and without micro Fe_3O_4 pigments and used as-is. In this phase, fig leaves extract at 1000 ppm concentration was incorporated into the

water-based Zinc Phosphate coating using mechanical stirring at 1000 rpm for 30 minutes.

Nano-structured Zinc Phosphate alkyd-based enamel coating was prepared by loading 1% wt. of Fe_3O_4 nano-powder slowly added to the alkyd resin and ground at high speed disperse for 30 min. Other pigments were then added and ground at high speed disperse to 4+ NS Hegman grind. Solvent and other additives were added as per the formulation. Another nanostructured alkyd-based enamel coating sample was prepared in the same manner, but with the use of glass beads during the grinding stage.

For Zinc Phosphate water-based acrylic coating, an aqueous dispersion of Fe_3O_4 was first formulated by adding 25 grams of DISPERBYK-2015 into 75 grams of double distilled water and mixing at 1000 rpm for 15 minutes. Five grams of Fe_3O_4 nano-powder were added slowly to the solution and the mixer speed was increased up to 10000 rpm and maintained for 30 minutes. The resultant slurry was then put into an ice bath and sonicated at 40% amplitude and 1 second on off pulse mode for 30 minutes. The dispersion was then added at the end of the grinding stage of the water-based acrylic coating followed by the rest of additives and fillers.

Prior to coating, the panels were degreased and prepared as per ASTM D609. Coatings were then sprayed to a Wet Film Thickness (WFT) of 150 µ to the mild steel panels measuring 150mm x 100mm x 0.8mm. Coated panels were then left to air dry for seven days before testing.

3.3 Characterization and Corrosion Tests

Prior to incorporating the Fe_3O_4 nano-powder into the different coatings, the powder particles were investigated by the X-Ray Diffraction technique for confirmation of their size. The elemental composition of the prepared coatings was determined using the X-Ray Fluorescence technique. The distribution of nano-particles in the coating was determined using the Scanning Electron Microscopy (SEM) technique. Electrochemical Impedance Spectroscopy (EIS) measurements were done for three replicates of each coated sample using a three-electrode cell. The coated panels with an exposed area of approximately 30.2 cm^2 served as the working electrode, Saturated Calomel (SC) as reference electrode, and a platinized titanium as auxiliary electrode. Figure 1 represents the test setup for the EIS study. The measurements were performed at room temperature in 0.5 M NaCl solution for periods up to 21 days. An electrochemical impedance measurement was performed under the open circuit

potential and in the frequency range of 0.3 Hz to 30 KHz with an applied AC signal of 10 mV amplitude. EIS spectra were developed using an automated single channel potentiostat. The impedance spectra for the different metal samples at different exposure times were analyzed and best fitted to the relevant equivalent circuit model shown in Figure 1 and Figure 2 respectively, using Zview™ software.

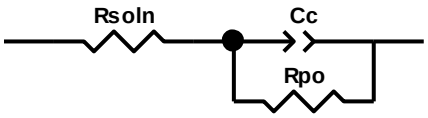

Figure 1. Randle's Equivalent circuit model for bare and coated metal samples with regular coating.

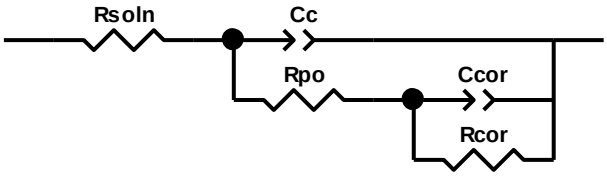

Figure 2. Equivalent circuit model for metal samples coated with nanostructured coating.

Chapter 4: Results and Data Analysis

4.1 Fig Leaves Extract

Fresh leaves of the fig plant were washed with tap water and dried using a fluidized bed dryer for one hour. After drying, the leaves were ground to fine particles. The leaves extract was then obtained using double distilled water and refluxing the solution for two hours to ensure complete extraction. After cooling, a vacuum filtration of the water-fig mixture was applied to retain the fig inhibitor extract. The concentration of the stock solution was determined to be approximately 14000 ppm.

The use of fig leaves extract as a corrosion inhibitor for bare mild steel in 0.5M NaCl solution and as an additive to a water-based coating has been investigated using electrochemical impedance spectroscopy over a frequency range between 0.03 Hz and 30 kHz and over a period of 21 days. The effect of adjusting the pH value of fig leaves extracts from pH=5.2 to pH=7 has also been looked into. Impedance measurements presented in the Nyquist and Bode plots for the average of three samples of mild steel immersed in 0.5M NaCl solution with and without corrosion inhibitors. Nyquist and Bode plots of mild steel in control solution are shown in Figure 3 through Figure 5.

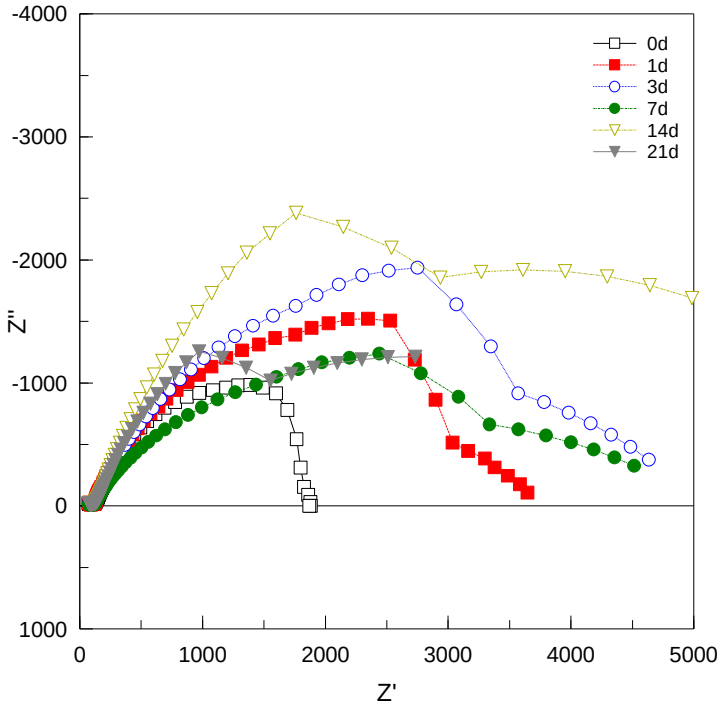

Figure 3. Nyquist plot of control over 21 days in 0.5 molar NaCl solution

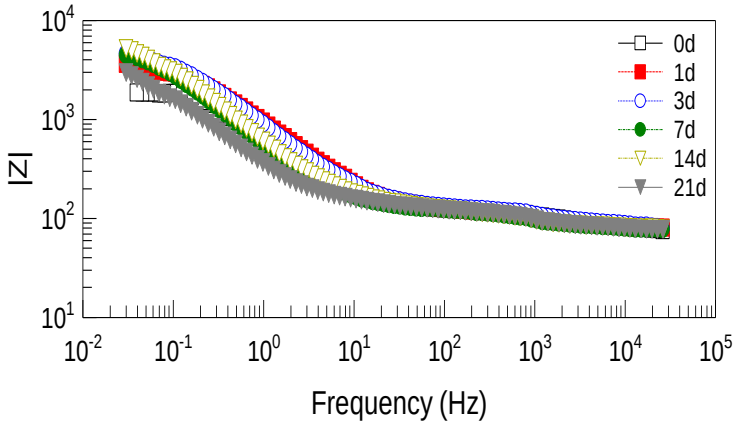

Figure 4. Impedance plot of control over 21 days in 0.5 molar NaCl solution

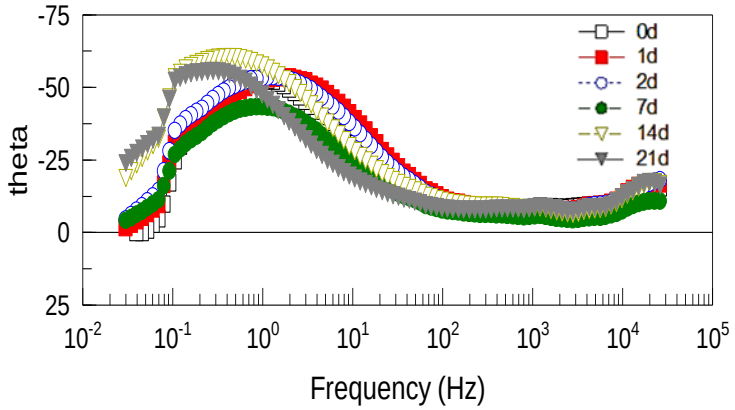

Figure 5. Phase plot of control over 21 days in 0.5 molar NaCl solution

The addition of fig leaves extract resulted in an increase in the diameter of Nyquist plots, but did not change their semicircle profile as shown in Figure 6 through Figure 8. This increase is attributed to the charge transfer resistance R_{ct} being the controlling factor in the corrosion of the steel substrate. Therefore, the inhibition efficiency was calculated using the charge transfer resistance as shown in equation (1).

$$IE\% = \frac{R_{ct} - R_{ct}^{\circ}}{R_{ct}} \times 100 \qquad (1)$$

The addition of fig leaves extract at 1000 ppm concentration has resulted in a reduction in the corrosion rate of bare mild steel. This decrease in the corrosion rate can be attributed to the adsorption of the inhibitor molecules onto the metal surface and the formation of a protective barrier of one or several molecular layers. This protective

molecular layer is believed to replace water molecules and decrease the diffusion rate of the reactant elements into the metal surface. It is also believed that this layer changes and suppresses the kinetics of cathodic and anodic reactions[37]. It is also worth mentioning that the inhibition effect of the extract appeared to be stable over the three-week period. Table 1 summarizes the evolution of electrical elements of Randel's equivalent circuit and inhibitor efficiency over 21 days period

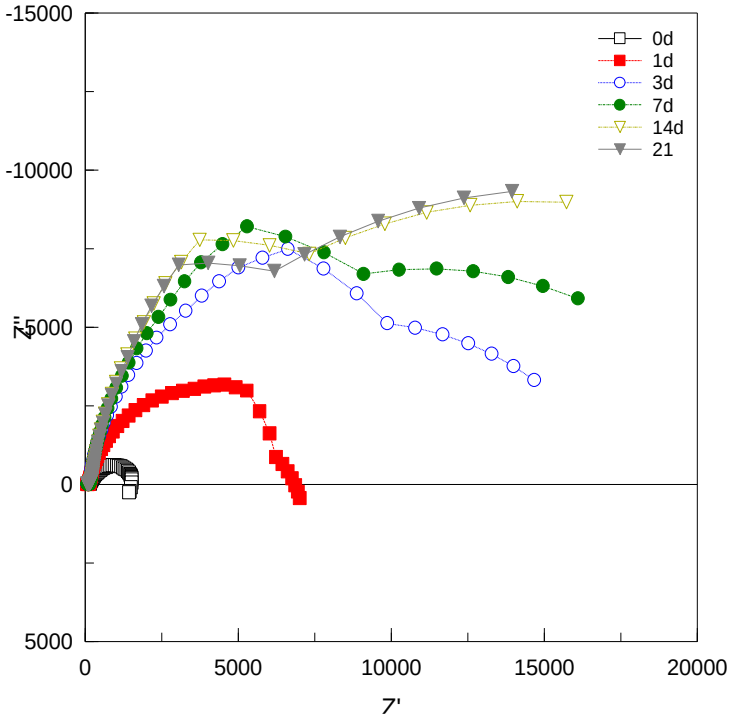

Figure 6. Nyquist plot for bare mild steel in 0.5 molar NaCl solution with fig leaves extract at 1000 ppm concentration over 21 days

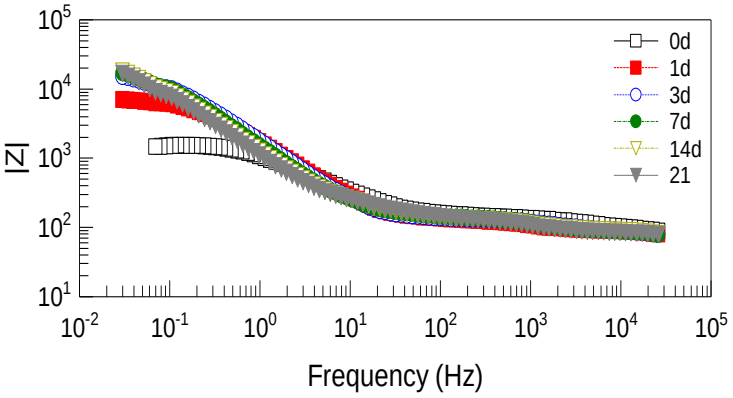

Figure 7. Impedance plot for bare mild steel in 0.5 molar NaCl solution with fig leaves extract at 1000 ppm concentration over 21 days

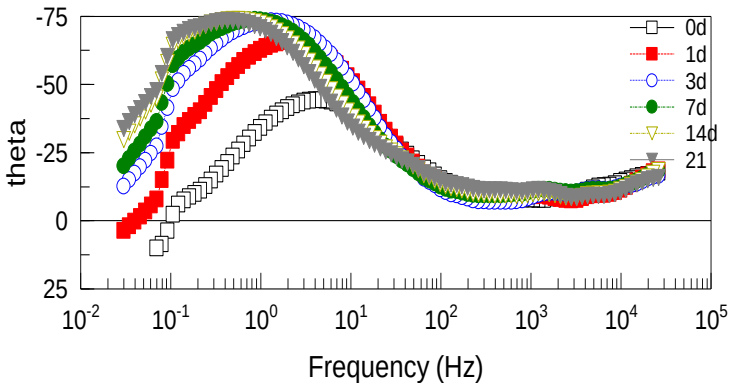

Figure 8. Phase plot for bare mild steel in 0.5 molar NaCl solution with fig leaves extract at 1000 ppm concentration over 21 days.

Table 1. *Evolution of Electrical Elements of Randle's Equivalent Circuit for Fig Leaves Extract in 0.5 Molar NaCl Solution over 21 Days*

	Time	**C_c (F/cm^2)**	**R_{ct} (Ω cm^2)**	**IE%**
Control	0 day	2.38E-04	1651	-
	1 day	1.35E-04	2661	-
	3days	1.53E-04	3242	-
	7 days	2.64E-04	2700	-
	14 days	2.80E-04	3825	-
	21 days	5.78E-04	2071	-
Fig leaves extract @ 1000 ppm	0 day	6.89E-05	3220	49%
	1 day	8.19E-05	5715	53%
	3days	8.77E-05	12345	74%
	7 days	1.05E-04	13834	80%
	14 days	1.27E-04	14178	73%
	21 days	1.47E-04	12725	84%
Fig leaves extract @ 1000 ppm adjusted pH to 7	0 day	2.05E-04	4620	64%
	1 day	1.18E-04	11949	78%
	3days	4.41E-05	18996	83%
	7 days	5.03E-05	25952	90%
	14 days	6.74E-05	29895	87%
	21 days	8.32E-05	26691	92%

The impact of adjusting the pH value of fig leaves extract to pH=7 was positive where it showed higher inhibition efficiency compared to untreated extract, as shown in Table 1. The Nyquist plot and Bode plots shown in Figure 9 through Figure 11 also concur with this finding. For example, Nyquist plot in Figure 9 shows a larger diameter for the different semicircles over the 21 days. On the other hand, Impedance plot in Figure 10 shows higher impedance values at the low frequency limit compared to those of the untreated extract.

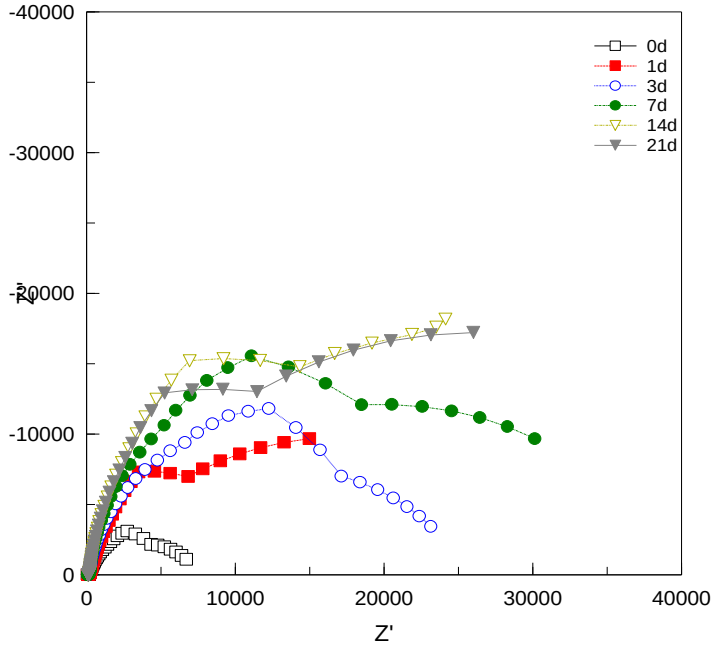

Figure 9. Nyquist plot for bare mild steel in 0.5 molar NaCl solution with fig leaves extract adjusted pH at 1000 ppm concentration over 21 days

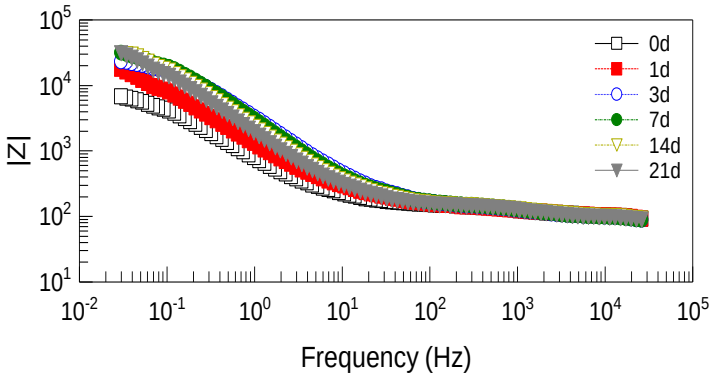

Figure 10. Impedance plot for bare mild steel in 0.5 molar NaCl solution with fig leaves extract adjusted pH at 1000 ppm concentration over 21 days

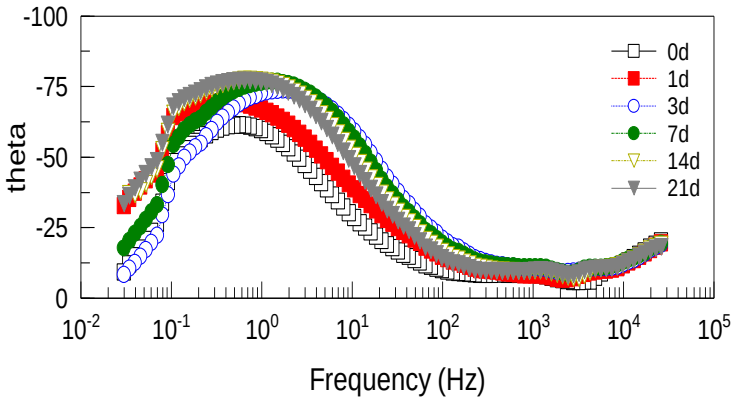

Figure 11. Phase plot for bare mild steel in 0.5 molar NaCl solution with fig leaves extract adjusted pH at 1000 ppm concentration over 21 days

The use of pH-adjusted fig leaves extract as an additive to the 0.5M NaCl solution and its positive impact on reducing the corrosion rate of the immersed substrate has led to examining its effect as an additive into water-based acrylic coating. The fig extract was incorporated into the coating during the grinding phase. The infused coating was then applied to mild steel plates at a coating thickness of 150µ WFT and its performance was compared to neat coating and coating pigmented with micro Fe_3O_4 powder using electrochemical impedance spectroscopy. Impedance measurements for the impregnated coat presented in the Nyquist plot and Bod plots in Figure 12 through Figure 14 indicate a better performance than the control coat shown in Figure 15 through Figure 17. This is demonstrated by the larger diameter of Nyquist semicircles and higher impedance values at the low limit frequencies in the impedance plots.

Figure18 through Figure 20 show the positive impact of micro Fe_3O_4 powder in the coating. The coating with fig leaves extract and micro iron oxide powder showed better R_{po} values than that of the control. They also both showed lower values for C_c compared to the control coating, indicating that both fig leaves extract and micro iron oxide powder demonstrated a corrosion inhibitive effect as shown in Table 2. The inhibitive effect of the micro iron oxide can be attributed to improving the barrier properties of the coating by physically separating the metallic substrate from the corrosive medium. However, the fig leaves extract is believed to provide corrosion protection by decreasing the activity of both anodic and cathodic reactions by releasing passivating ions[38].

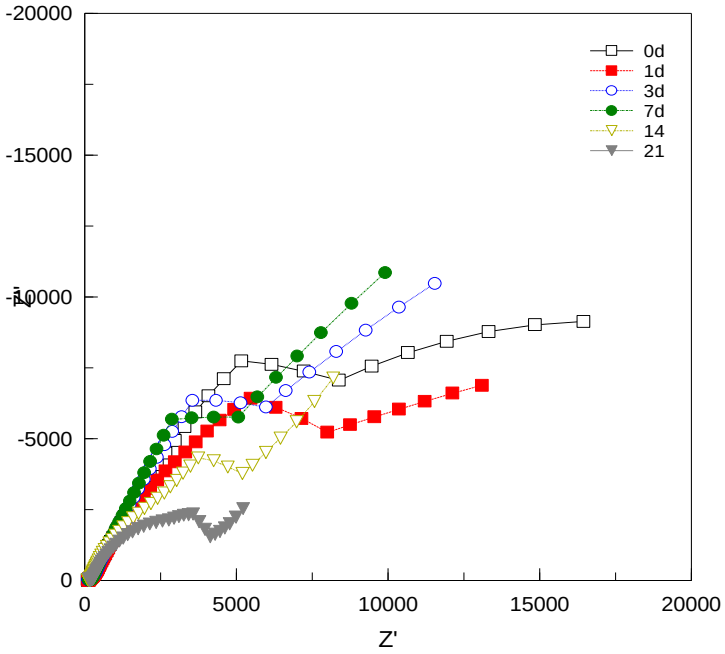

Figure 12. Nyquist plot of mild steel coated with water based acrylic coating with fig leave extract immersed in 0.5 molar NaCl solution

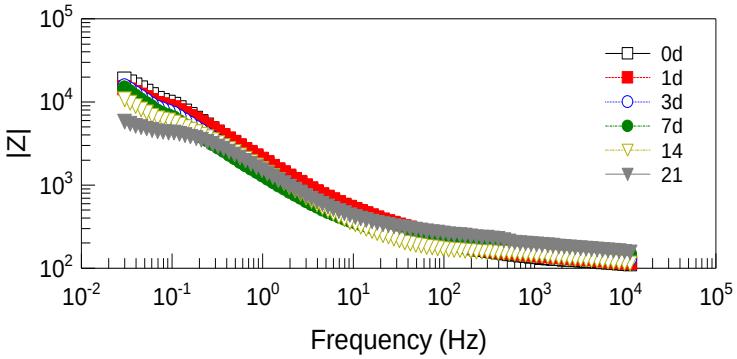

Figure 13. Impedance plot of mild steel coated with water based acrylic coating with fig leave extract immersed in 0.5 molar NaCl solution

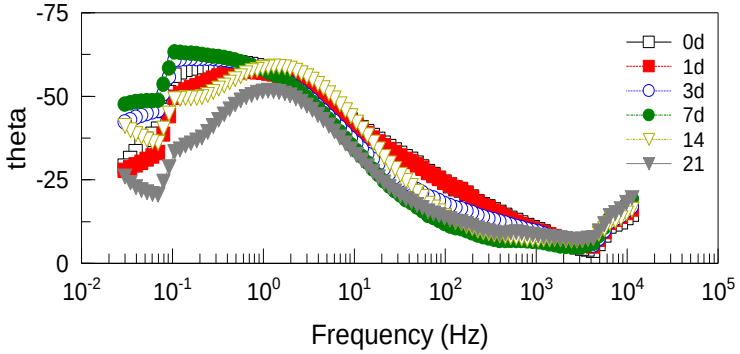

Figure 14. Phase plot of mild steel coated with water based acrylic coating with fig leave extract immersed in 0.5 molar NaCl solution

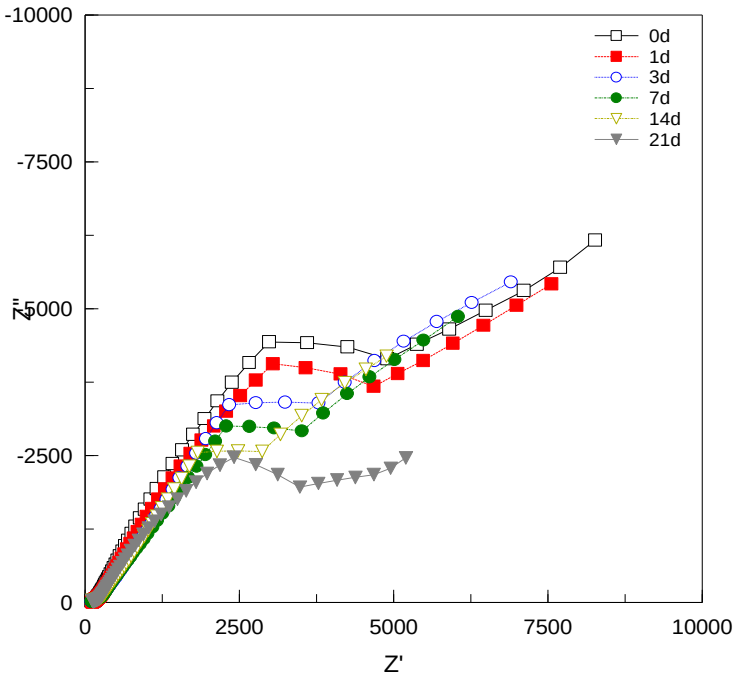

Figure 15. Nyquist plot of mild steel coated with control water based acrylic coating immersed in 0.5 molar NaCl solution

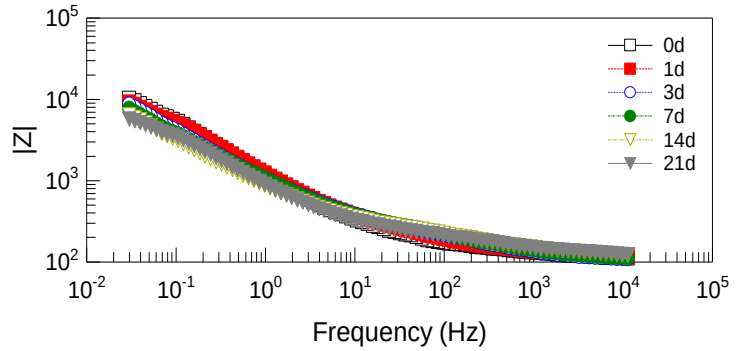

Figure 16. Impedance plot of mild steel coated with control water based acrylic coating immersed in 0.5 molar NaCl solution

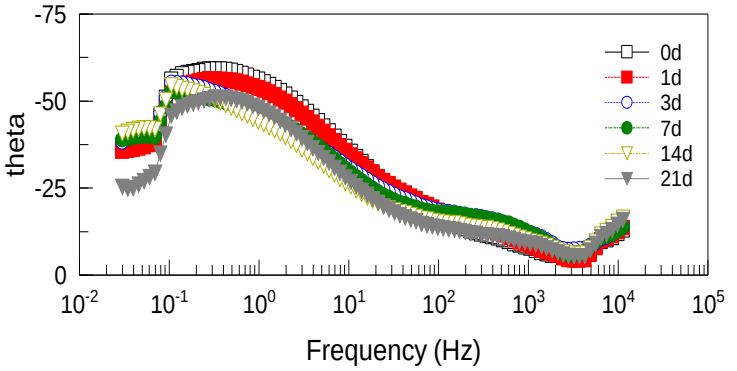

Figure 17. Phase Plot of mild steel coated with control water based acrylic coating immersed in 0.5 molar NaCl solution

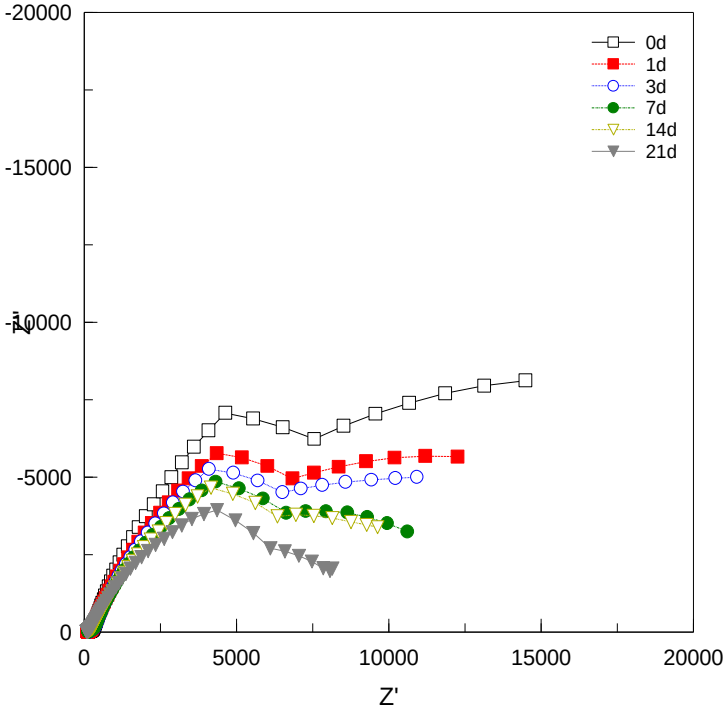

Figure 18. Nyquist plot of mild steel coated with water based acrylic coating with micro iron oxide powder immersed in 0.5 molar NaCl solution

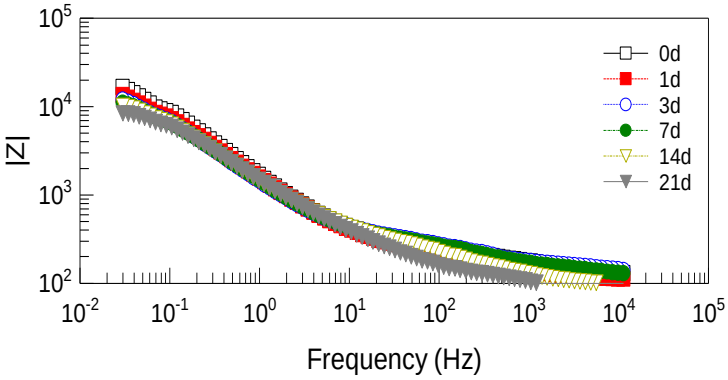

Figure 19. Impedance plot of mild steel coated with water based acrylic coating with micro iron oxide powder immersed in 0.5 molar NaCl solution

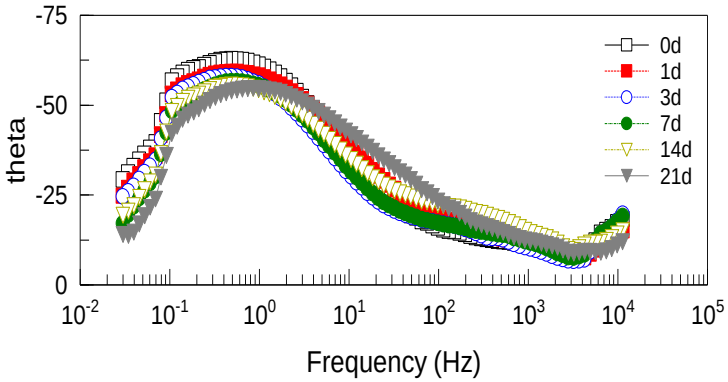

Figure 20. Phase plot of mild steel coated with water based acrylic coating with micro iron oxide powder immersed in 0.5 molar NaCl solution

Table 2. *Evolution of Electrical Elements of Randle's Equivalent Circuit for Water-based Coating with Fig Leaves Extract and Micro Iron Oxide in 0.5Molar NaCl Solution over 21 Days*

	Time	**C_c (F/cm^2)**	**R_{ct} (Ω cm^2)**
Control Coating	0 day	1.27E-04	7441
	1 day	1.10E-04	6146
	3days	1.28E-04	4999
	7 days	1.29E-04	4316
	14 days	1.77E-04	3733
	21 days	1.59E-04	3614
Coating with Fig leaves extract and mirco Iron Oxide	0 day	6.20E-05	11867
	1 day	5.67E-05	9188
	3days	9.45E-05	10171
	7 days	1.23E-04	10339
	14 days	9.28E-05	7561
	21 days	8.14E-05	3512

4.2 Characterization of Nano-Fe_3O_4 Particles

Figure 21 shows the X-Ray Diffraction of nano-Fe_3O_4 powder and confirms the crystallinity of iron oxide. Applying Scherrer Equation (2) at peak number 388 with 2θ=35.42°, β=0.62, K=0.9, and λ $Cuk_{\alpha 1}$=0.154060 nm, the calculated size was 13.45 nm [39]. Please note that β and θ should be converted to radians.

$$L = \frac{0.9\,\lambda_{K\alpha 1}}{\beta_{(2\theta)}\,\cos\theta} \qquad (2)$$

Where λ is the X-ray wavelength in nanometer, β is the peak width of the diffraction peak profile at half maximum height resulting from small crystallite size in radians, and K is a constant related to crystallite shape, usually taken as 0.9.

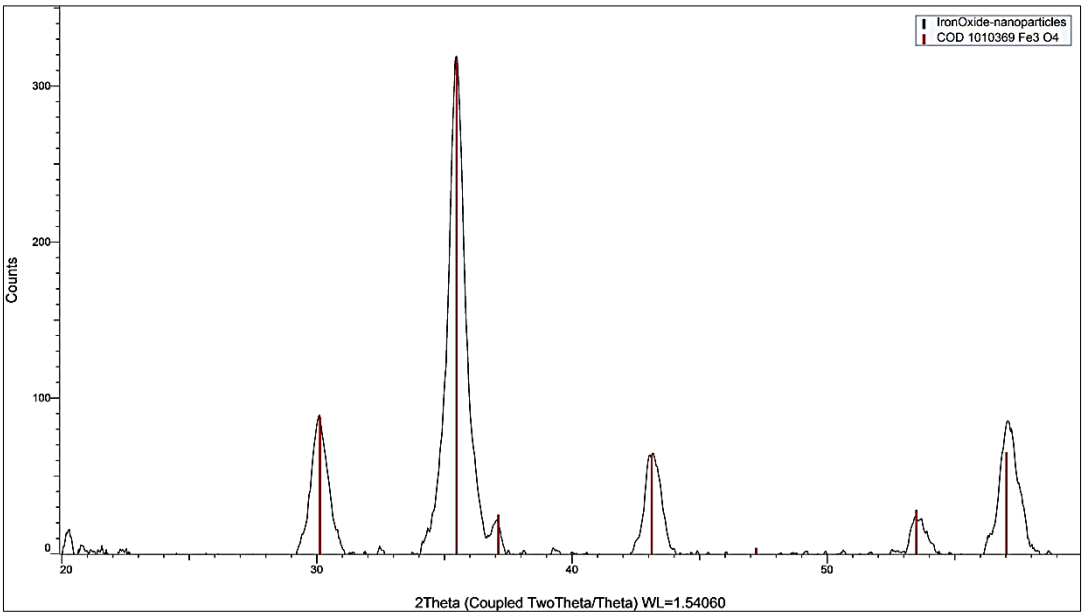

Figure 21. X-ray diffraction patterns of nano-Fe3O4 powder.

4.3 Zinc Phosphate Alkyd-based Enamel Coating

4.3.1 Coating characterization using XRF technique.

A Horiba X-ray analytical microscope, with X-Ray diameter of 1.2mm, X-ray tube voltage of 50 kV, and 1 mA current, was used to acquire the XRF spectra for all the different coating samples. Table 3 summarizes the XRF elemental analysis for the alkyd-based enamel coating. By comparing the control samples and the nano-modified ones, the presence of iron particles from Fe_3O_4 is confirmed.

Table 3. *XRF Elemental Analysis for Alkyd-based Coating*

	Al	P	Ca	Ti	V	Fe	Zn	Sr	Zr	Pb	S
Control coating	0.32	3.33	79.38	3.75	0.09	0.14	12.38	0.05	0.05	0.36	0.00
Nano-modified Coating	0.33	3.12	76.53	6.32	0.17	0.90	12.320	0.06	0.05	0.19	0.00

4.3.2 Electrochemical impedance spectroscopy.

The different samples were immersed in 0.5 M NaCl solution and impedance spectra were collected at different points in time: one day, two days, seven days, fourteen days, and twenty one days. At the end of the immersion period, the coating-exposed area was photographed before and after the removal of the coating layer. The

impedance spectra of all the different coated samples indicate that the impedance modulus |Z| decreases with the immersion time. This in turn confirms the ability of EIS to detect the changes that occur in the samples during the degradation process. The average data from three samples of each coating category was analyzed and best fitted to the equivalent circuit shown previously in Figure 2.

The selection of the equivalent circuit was based on the Nyquist plots that showed the development of two semicircles on the second day. In the equivalent circuit of, Rsoln represents electrolyte resistance; that is, the resistance between the working electrode and the reference electrode. Rsol is generally small and can be neglected. Cc is the capacity of the coating film and it was molded as a constant phase element to reflect the non-ideal behavior. Rpor is the pore resistance related to the permeability and the formation of ionically conducting paths in the coating. The second time constant of the spectra represents the electrochemical process, taking place at the metal-coating interface. Hence, Ccor is the double-layer capacitor and can be used as a measure of the paint's loss of adhesion. It was modeled after a constant phase element to represent the non-ideal behavior of the capacitor. Rcor denotes the charge transfer resistance associated with the kinetic of the corrosion process. In this work, Rcor and |Z| at the lower limit of frequency range will be used to compare the protective properties of the coatings. The increase in Cc and the resulting water uptake will also be used to indicate the degree of the degradation of the coating. The water content will be calculated using the Brasher and Kingsbury formula shown in equation (3).

$$\phi = \frac{\log(C_{ct}/C_{co})}{\log \varepsilon_{water}} \qquad (3)$$

Where C_{ct} is the coating's capacitance at any time, C_{co} is the initial capacitance at time zero and ε_{water} the dielectric constant of water at the working temperature; and Ø is the water content expressed as volume fraction in the coating. At ambient temperature of 293-298K and a dielectric constant of water of 80.2 was used.

4.3.2.1 Control Zinc Phosphate alkyd-based enamel coating.

At zero time the impedance modulus |Z| at the low-frequency limit displayed a high average value of 2.17E+8 $\Omega.cm^2$. Only one time constant could then be detected from the inspection of the Nyquist plot in Figure 21, which was responsible for the barrier characteristic of the coating[40]. However, as the electrolyte solution increasingly penetrated the coating in the following 48 hours, capacitive behavior in the

Bode diagram was observed; the maximum phase angle at the high frequency limit showed lower average values of 56° after one day and 43° after two days as shown in phase plot in Figure 23. At the same time, a continuous decrease in the value of the impedance modulus |Z| at the low-frequency limit took place, with average values of 1.57E+7 $\Omega.cm^2$ and 2.3E+6 $\Omega.cm^2$ after one day and two days respectively, as shown in the impedance diagram in Figure 24. Such early signs indicated degradation in the protective properties of the control Zinc Phosphate alkyd-based enamel coating [83-84].

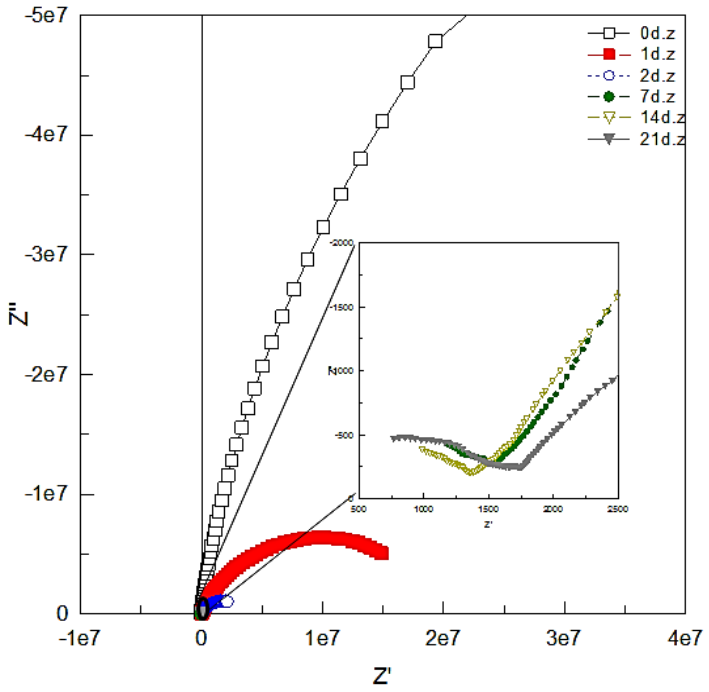

Figure 22. Nyquist plot of control Zinc Phosphate enamel coating immersed in 0.5 molar NaCl solution

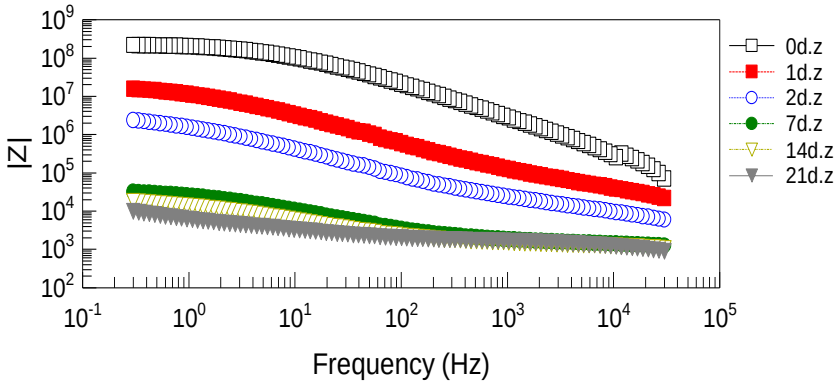

Figure 23. Impedance plot of control Zinc Phosphate enamel coating immersed in 0.5 molar NaCl solution

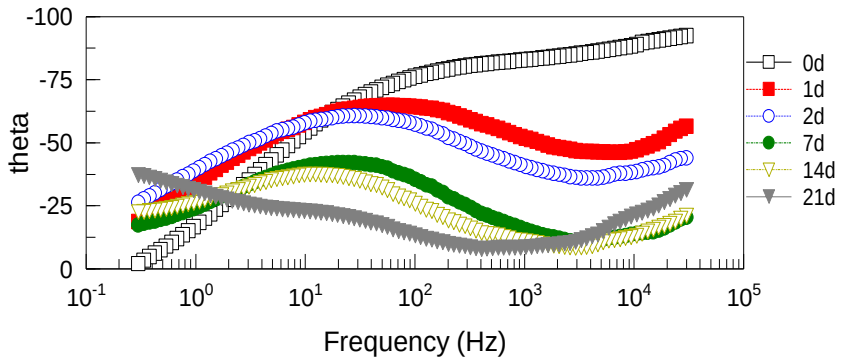

Figure 24. Phase plot of control Zinc Phosphate enamel coating immersed in 0.5 molar NaCl solution

The close-up view in the Nyquist plot in Figure 22 shows the development of the second time constant in the Nyquist plot, which started to show clearly at seven days. At this time, the insulation effect of the film was somewhat lost in random areas, letting the metal substrate come in direct contact with the electrolyte[41]. This eventually allowed the corrosion process to commence at the interface between the metal surface and the coating in the defected areas. This process is represented by the change in resistance in the charge transfer process between the metal and the electrolyte, which is in our case the R_{cor}. The comparative decrease in impedance modulus |Z|, pore resistance R_{por}, and charge transfer resistance R_{cor} after seven days of immersion were suggestive of high permeability of the electrolyte to the coating[42]. This was also confirmed by the clear presence of the second time constant in the Nyquist plot and the water uptake volume (Ø) calculated at seven days compared to one day immersion [86-87]. Subsequently, the impedance modulus |Z| and all other parameters continue to change unfavorably until the end of immersion at 21 days as shown in Table 4. The change in water uptake (Ø) and R_{cor} values during the immersion period are shown in Figure 25 and Figure 26, respectively.

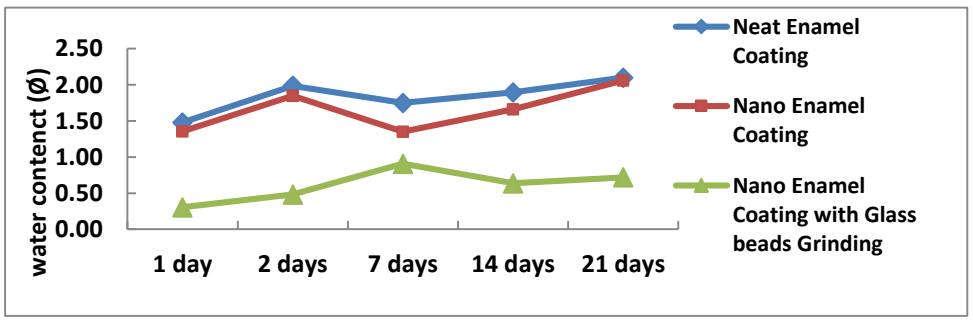

Figure 25. Water uptake (Ø) during 21 days of immersion in 0.5 molar NaCl solution for the different coatings.

Table 4. Evolution of Electrical Elements from Equivalent Circuit of Alkyd-based Enamel Coatings

	Time (days)	C_c (F/cm^2)	R_{po} (Ω cm^2)	C_{Cor} (F/cm^2)	R_{Cor} (Ω cm^2)
Standard	0 day	1.49E-11	8.52E+05	3.14E-10	2.44E+08
Enamel	1 day	9.72E-09	1.29E+05	3.86E-09	1.92E+07
Coating	2 days	8.98E-08	2.76E+04	4.40E-08	3.57E+06
	7 days	3.19E-08	1.22E+03	6.06E-06	3.76E+04
	14 days	6.01E-08	1.17E+03	1.45E-05	2.32E+04
	21 days	1.48E-07	1.45E+03	3.40E-05	7.14E+03
Nano	0 day	1.76E-12	4.27E+05	3.43E-10	9.75E+08
Enamel	1 day	6.65E-10	1.42E+06	2.40E-09	1.58E+07
Coating	2 days	5.78E-09	1.57E+04	1.14E-07	5.68E+05
	7 days	6.56E-10	1.61E+03	1.22E-05	1.04E+05
	14 days	2.54E-09	1.34E+03	5.51E-05	6.78E+04
	21 days	1.46E-08	1.38E+03	2.08E-05	2.00E+04
Nano	0day	1.35E-10	8.79E+06	1.05E-09	1.22E+09
Enamel	1 day	5.14E-10	7.08E+04	1.45E-06	1.45E+08
coating	2 days	1.11E-09	3.95E+04	7.54E-06	2.39E+07
with	7 days	7.20E-09	2.53E+04	9.11E-06	1.42E+05
Glass	14 days	2.19E-09	2.58E+04	7.22E-06	3.11E+05
beads	21 days	3.14E-09	2.24E+04	1.66E-05	4.95E+05

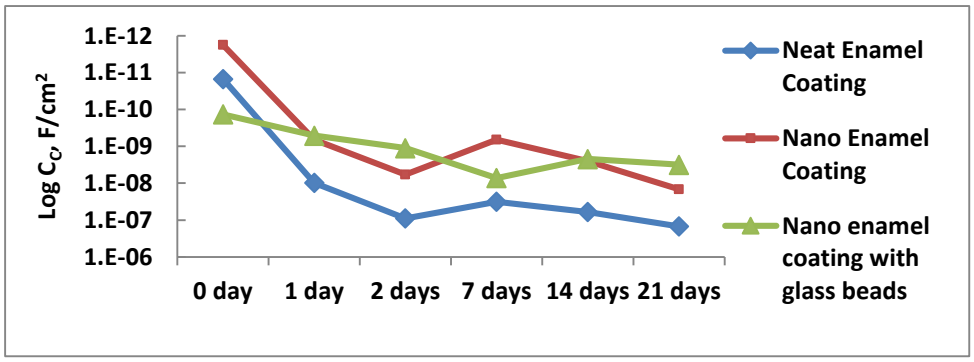

Figure 26. Change in coating capacity during 21 days of immersion in 0.5 molar NaCl solution for the different coatings.

4.3.2.2 Fe_3O_4 nano-modified Zinc Phosphate enamel coating.

As shown in Figure 27, the impact of incorporating 1% wt. nano-Fe_3O_4 particles resulted in an increase in the impedance modulus at the low-frequency limit $|Z|_{0.3\ Hz}$ to an average value of 9.00E+8 Ω.cm^2[43]. As immersion continued, the penetration of the corrosive electrolyte into the coating increased in the following 48 hours, the capacitive behavior in the Bode diagram was observed; the maximum phase angle at the high frequency limit showed lower average values of 80° and 44° as shown in phase plot in Figure 28, which are higher than the values of the control enamel coating[41]. At the same time, a continuous decrease in the value of the impedance modulus |Z| at the low-frequency limit took place[43], with average values of 1.65E+7 Ω.cm^2 and 9.00E+5 Ω.cm^2.

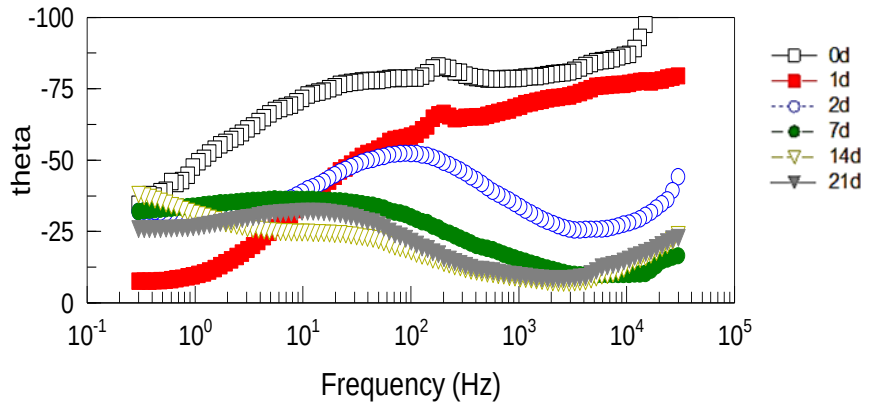

Figure 27. Phase plot of nano modified Zinc Phosphate enamel coating immersed in 0.5 molar NaCl solution

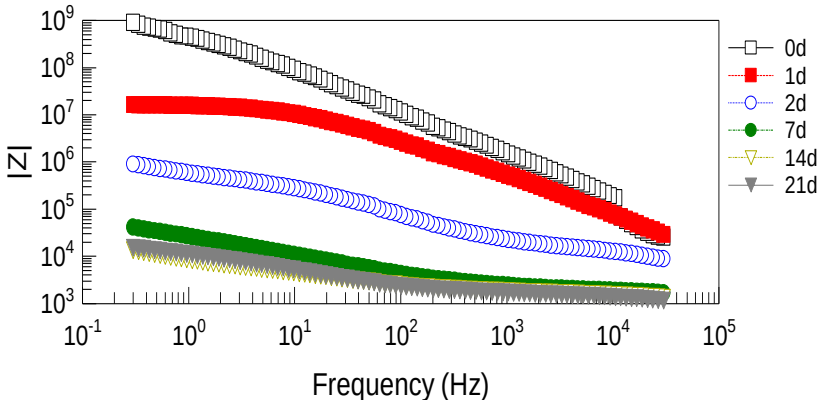

Figure 28. Impedance plot of nano modified Zinc Phosphate enamel coating immersed in 0.5 molar NaCl solution

The zoomed-in view in the Nyquist plot is shown in Figure 29. It also shows the development of two time constants in the Nyquist plot, which started to be prominent at seven days. However, by comparing the values of the different parameters in Table 4, it might be concluded that the nano-modified coating has better corrosion resistance properties than the standard one. This can also be concluded by comparing the water uptake and C_c values in Figure 25 and Figure 26, respectively [86-87].

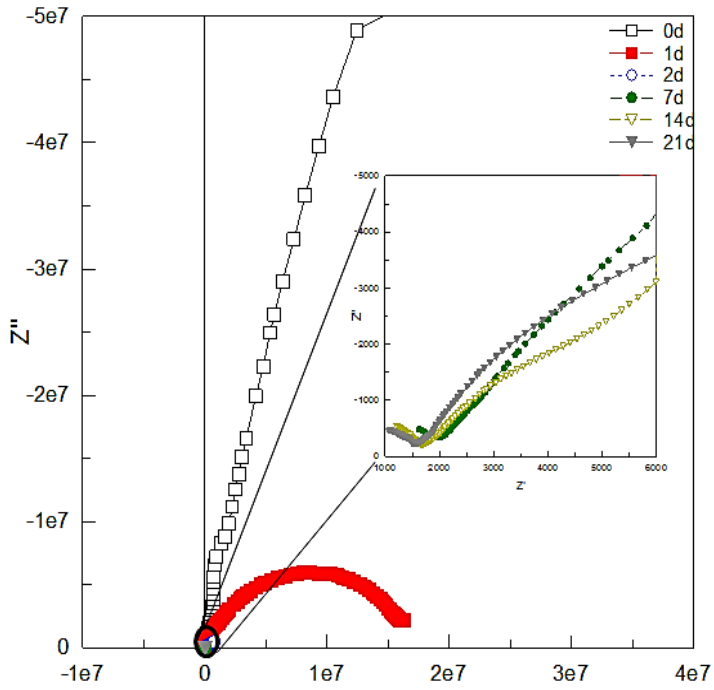

Figure 29. Nyquist plot of nano modified Zinc Phosphate enamel coating immersed in 0.5 molar NaCl solution

4.3.2.3 Fe_3O_4 nano-modified Zinc Phosphate enamel coating prepared with glass beads during the grinding stage.

This coating showed a different behavior compared to former coatings. Figure 30 shows a lower impedance modulus $|Z|_{0.3\ Hz}$ after one day and two days. However, this trend was reversed after seven days of immersion, showing 153% and 96% higher $|Z|_{0.3\ Hz}$ values than control and nano-modified coatings. At 21 days, the impact was even more dominant, showing 483% and 275% higher $|Z|_{0.3\ Hz}$ values than the control and nano-modified coatings, respectively [32].This was also confirmed by the sudden change in the rate of change in R_{cor} values at the 7th day[38]. The use of glass beads during the grinding phase of the coating resulted in an R_{cor}, after 21 days that is 2373%

and 6832% higher than the control and nano-modified coating, respectively as shown in Table 4. It also led to lower water uptake values during the 21-day immersion period, an average of 35% reduction in the water uptake compared to the other two coatings as shown in Figure 25.

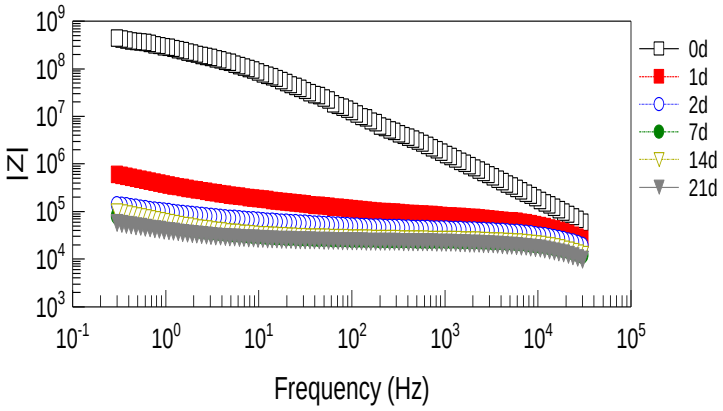

Figure 30. Impedance plot of Fe3O4 nano-modified Zinc Phosphate enamel coating prepared with glass bead immersed in 0.5 molar NaCl solution

Figure 31. shows surface condition of the exposed area immediately after the 21-days immersion. The surface for nano-modified Zinc Phosphate enamel coating prepared with glass bead shows less corrosion products and discoloration. It was also noticed that it was more difficult to remove this coating compared to the other two coatings, which might indicate better adhesion. Such behavior can be attributed to the assumption that by using glass beads during the grinding phase, we decrease the size of the nanoparticle agglomerates, resulting in better distribution across more surface area, leading to more resin being absorbed on their surfaces and reducing the interspaces that will eventually enhance the density of the coatings and reduce the transport paths that the corrosive electrolyte must pass through to the coating system[44]. Another observation is that it took this coating about one week to start to supersede the performance of the two other coatings. This might be attributed to a diffusion and redistribution process of the nano-particles in the coating matrix with time.

4.3.3 Scanning electron microscopy for alkyd-based coatings.

Figure 32. shows the SEM micrographs of unexposed samples of alkyd-based enamel coating. On the left is the control sample and on the right is the nano-modified alkyd-based enamel coating prepared with glass beads during the grinding stage. By comparing both micrographs, the coating prepared with glass beads shows a more

crystalline structure compared to the control sample. However, nothing much could be concluded about the microstructure or the presence of the nano-particles.

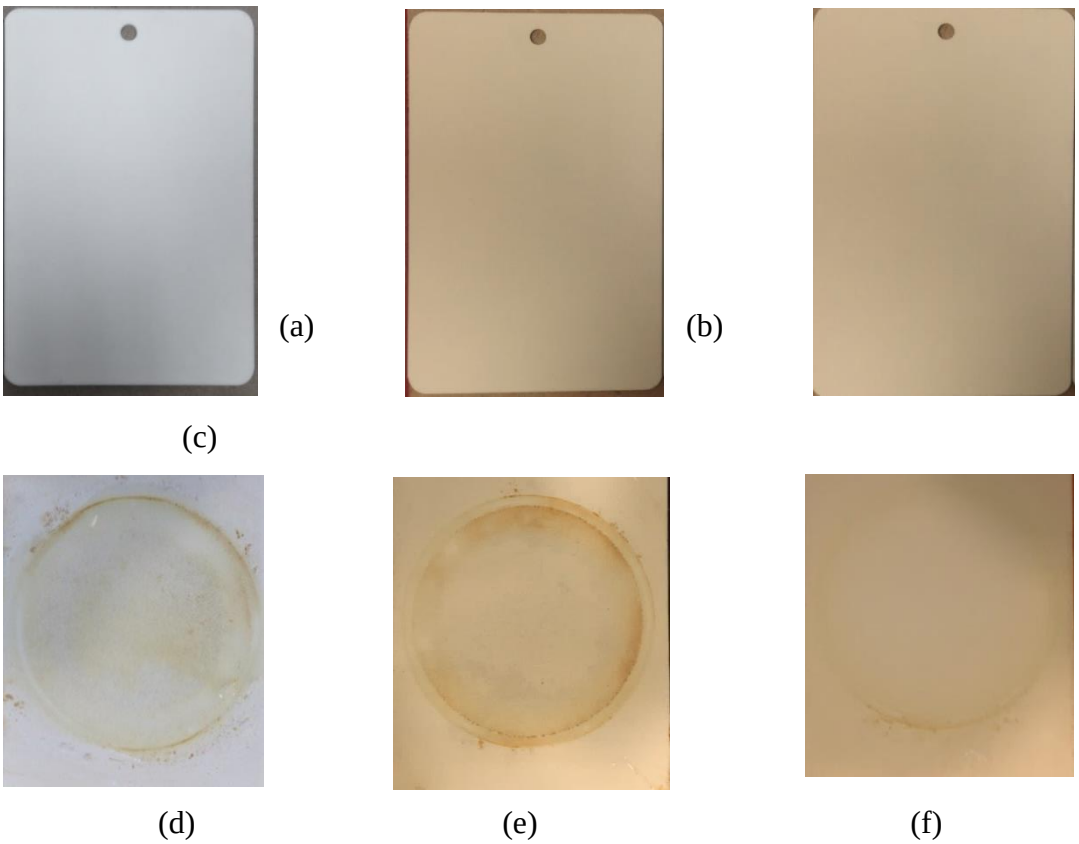

Figure 31. Enamel coating samples before and after EIS respectively (a) and (d) control; (b) and (e) nano-modified; and (c) and (f) nano-modified prepared with glass beads.

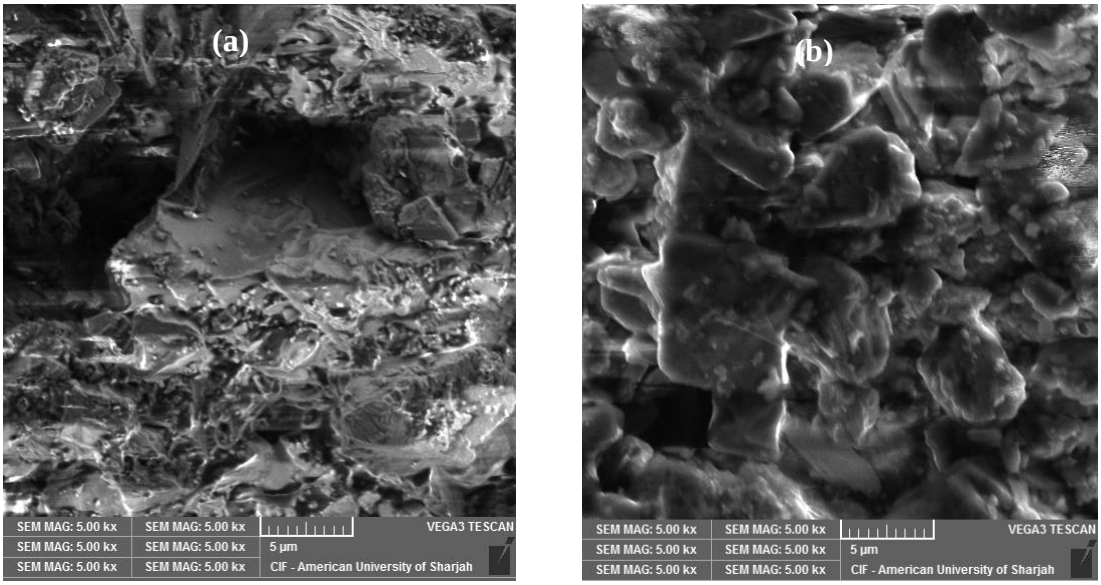

Figure 32. SEM surface morphology (a) unexposed control sample; (b) nano-modified alkyd-based enamel coating.

4.4 Zinc Phosphate Water-based Acrylic Coating

4.4.1 Coating characterization using XRF technique.

A Horiba X-ray analytical microscope, with X-Ray diameter of 1.2 mm, X-ray tube voltage of 50 kV, and 1 mA current, was used to acquire the XRF spectra for all the different coating samples. Table 5 summarizes the XRF elemental analysis for the alkyd-based enamel coating. By comparing the control samples and the nano-modified ones, the presence of iron particles from Fe_3O_4 is confirmed.

Table 5. *XRF Elemental Analysis for Water-based Coating*

	Na	Al	Si	P	S	K	Ca	Ti	Fe	Zn	Zr
Control coating	7.87	2.21	0.69	7.00	1.06	0.32	6.11	45.32	0.10	29.13	0.17
Nano-modified Coating	4.81	2.00	0.47	6.43	0.87	0.29	5.01	44.74	3.65	31.54	0.19

4.4.2 Electrochemical impedance spectroscopy.

The protective capacity of the water-based coatings was evaluated by observing the behavior of three replicates of neat coating and nano-modified coating samples in immersion tests, using the EIS technique. For this, the three electrochemical cells were used with an exposed area of 30.18 cm^2. The mild steel substrate served as the working electrode. A saturated calomel electrode was used as the reference electrode, and platinized titanium as the auxiliary electrode. An ACM Gill AC potentiostat was utilized to acquire the electrochemical measurements. Electrochemical impedance spectra were gathered over the course of 21 days for the coated samples, observing the degradation of the system over a maximum period of 230 days. The range of frequencies employed for recording the impedance spectra was from 1×10^{-3} Hz to 30 kHz, and the amplitude of the signal was 10 mV.

4.4.2.1 Neat Zinc Phosphate water-based acrylic coating.

Figure 33 through Figure 35 show the Nyquist and Bode plots for the neat Zinc Phosphate water-based acrylic coating. At zero time the impedance modulus |Z| at the low-frequency limit displayed an average value of 3.06E+3 $\Omega.cm^2$. Two time constants could be detected from the inspection of the Nyquist plot Figure 33, which is an indication of the poor barrier characteristic of the coating. The low value of $|Z|_{0.3Hz,}$ below 1E+6 $\Omega.cm^2$ as shown in Figure 34, and the presence of the two time constants in the Nyquist plot may direct us to conclude that the coating is not protecting the

substrate adequately [45]. Bethencourt, et al. [40] suggests that EIS technique does not become sensitive enough for detecting the start of the degradation process in coatings showing initial impedance values less than 1E+6 $\Omega.cm^2$. This might explain the difficulty in generating the best fit curves and obtaining the values for R_{cor} and C_{cor}. Therefore, an attempt was made to generate best fit using Randle's circuit in Figure 1.

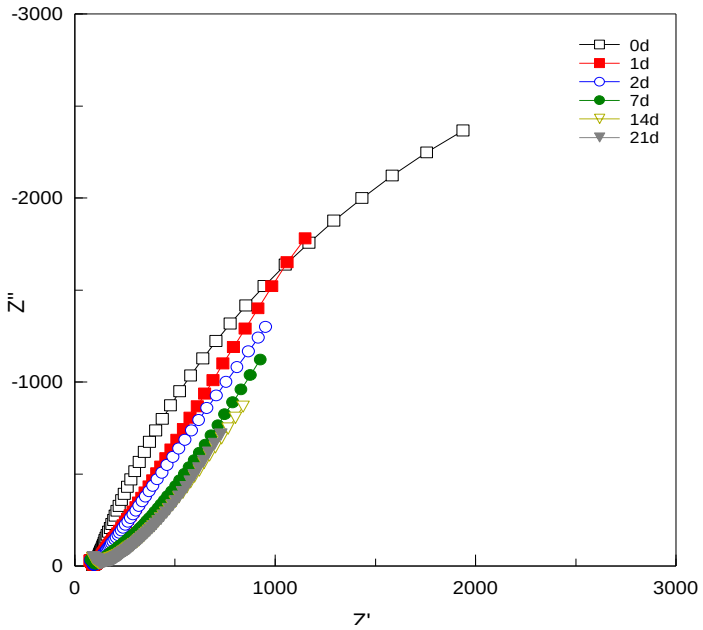

Figure 33. Nyquist plot of standard water based acrylic bead immersed in 0.5 molar NaCl solution

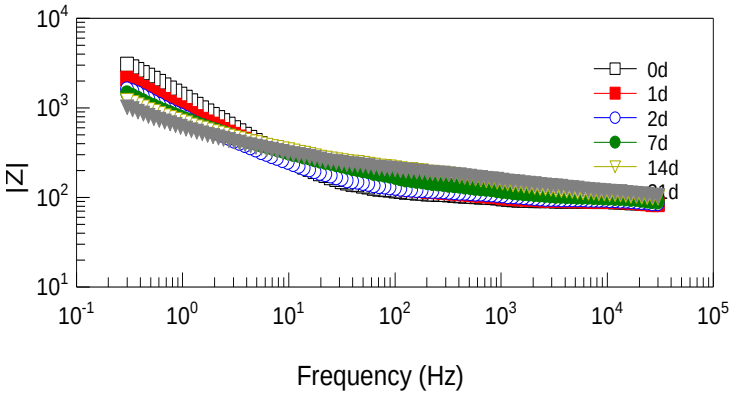

Figure 34. Impedance plot of standard water based acrylic bead immersed in 0.5 molar NaCl solution

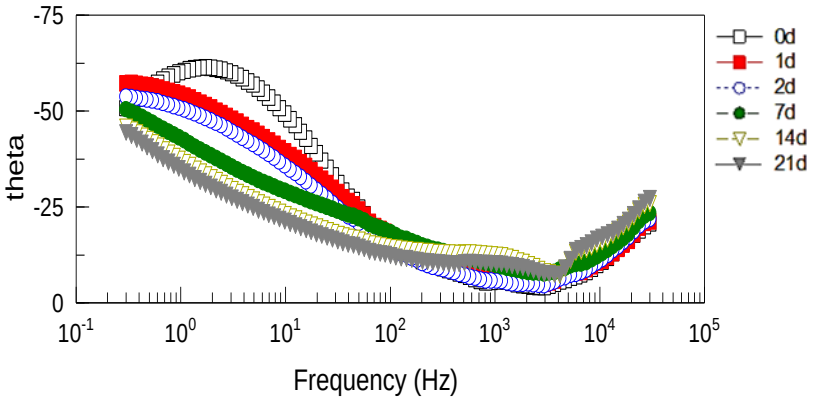

Figure 35. Phase plot of standard water based acrylic bead immersed in 0.5 molar NaCl solution

Table 6 summarizes the values for coating capacity, C_c, and the pore resistance, $R_{por,}$ for the neat water-based coating. The values show that the pore resistance is inversely proportional to the immersion period, where it continuous to decrease with time, indicating coating film. Another indication for the permeation of water is the increase in C_c values throughout the immersion time.

4.4.2.2.Fe_3O_4 nano-modified Zinc Phosphate water-based acrylic coating.

By comparing Figure 36 through Figure 38, which show the Bode and Nyqusit plots for the nano-modified Zinc Phosphate water-based acrylic coating to those of the standard coating and Table 6, we may be able to conclude that the addition of 1% wt Fe_3O_4 nano particles to the formulated water-based acrylic coating did not achieve the anticipated positive impact on the protection properties of the coating under consideration. This could be due to the fact that the standard coating matrix itself is weak to the extent that it does not allow the EIS technique to detect the changes.

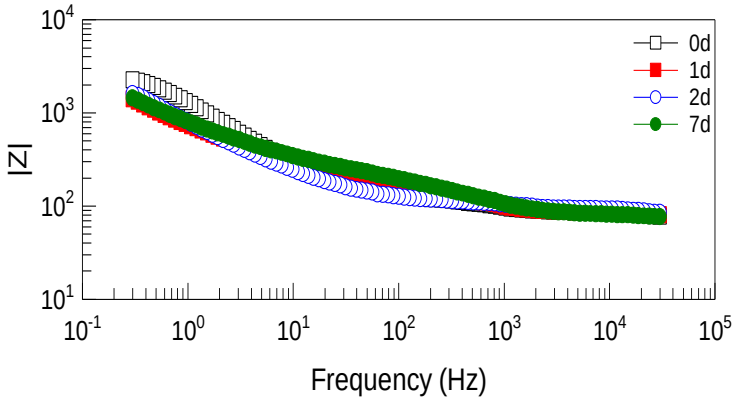

Figure 36. Impedance plot of nano- modified water based acrylic bead immersed in 0.5 molar NaCl solution

Table 6. *Evolution of Electrical Elements from Equivalent Circuit of Water-based Acrylic Coatings*

	Time (days)	C_c (F/cm^2)	R_{po} (Ω cm^2)
Standard Enamel Coating	0 day	8.81E-05	3.34E+03
	1 day	1.03E-04	1.93E+03
	2 days	1.14E-04	1.25E+03
	7 days	9.50E-05	9.67E+02
	14 days	1.23E-04	7.67E+02
	21 days	1.52E-04	6.54E+02
Nano-modified	0 day	7.85E-05	1.95E+03
water-based	1 day	7.60E-05	8.32E+02
coating	2 days	1.29E-04	1.46E+03
	7 days	6.36E-05	7.90E+02

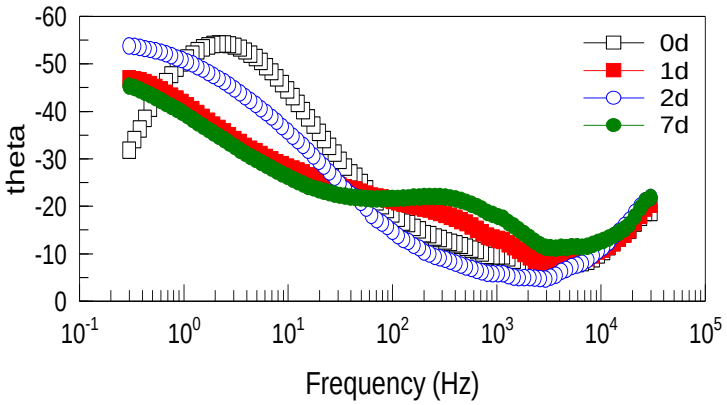

Figure 37. Phase plot of nano- modified water based acrylic bead immersed in 0.5 molar NaCl solution

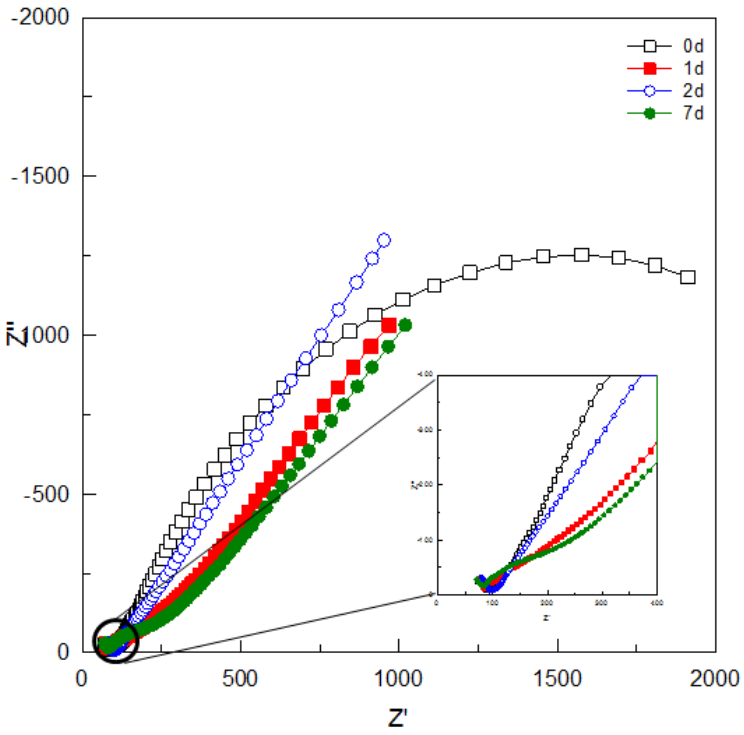

Figure 38. Nyquist plot of nano- modified water-based acrylic bead immersed in 0.5 molar NaCl solution

4.4.3 Scanning Electron Microscopy for water-based coatings

Figure 39. SEM surface morphology of unexposed control sample (a) water-based acrylic coating; (b) nano-modified water-based acrylic coating shows the SEM micrographs of unexposed samples of the water-based acrylic coating, for both the control and the nano-modified water-based acrylic coating. However, both images look similar and very little, if any; can be inferred about the presence and distribution of the nano-particles.

4.4.3.1 Nano-modified Zinc Phosphate water-based acrylic coating exposed to magnetic field.

Sabzi, and Dhoke stressed the importance of uniformly distributing the nano-particles in the coating matrix. The magnetic nature of Fe_3O_4 nano-particles created an interest in examining the effect of exposing those particles to a magnetic field and determining its effect on improving the barrier properties of the water-based acrylic coating [13] [32].

The first step was to study the effect of the magnetic field of a permanent magnet on the distribution of the nano-particles dispersed in water using an optical microscope. Figure 0 demonstrates the effect of the magnetic field on the distribution of the magnetic agglomerates, which clearly indicates the possibility of using the magnetic field to affect the distribution of the particles in the coating matrix. This can result in covering more surface area and reducing the ionic paths in the composite coating achieving a more protective coating.

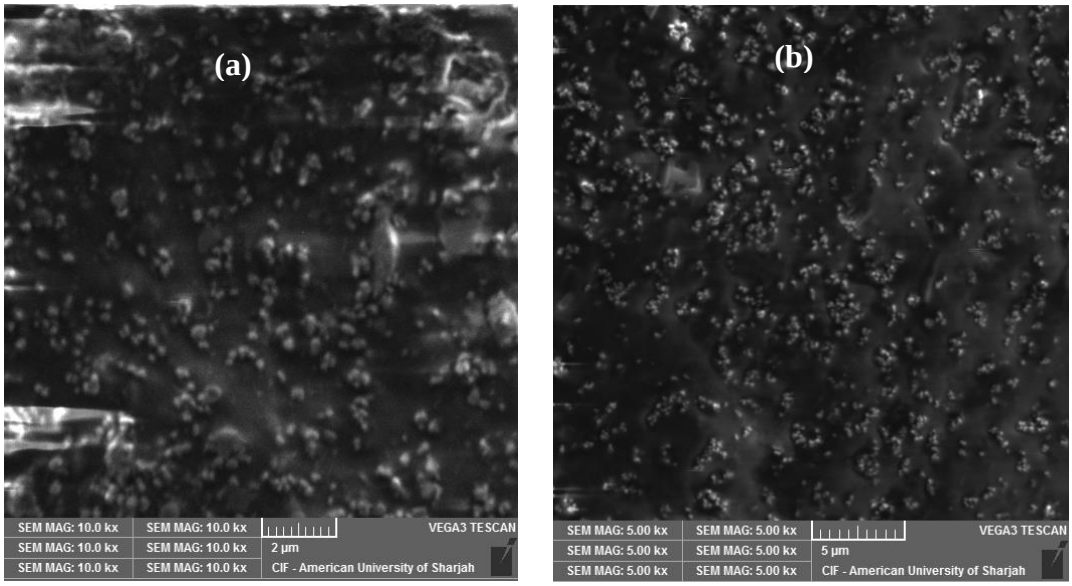

Figure 39. SEM surface morphology of unexposed control sample (a) water-based acrylic coating; (b) nano-modified water-based acrylic coating

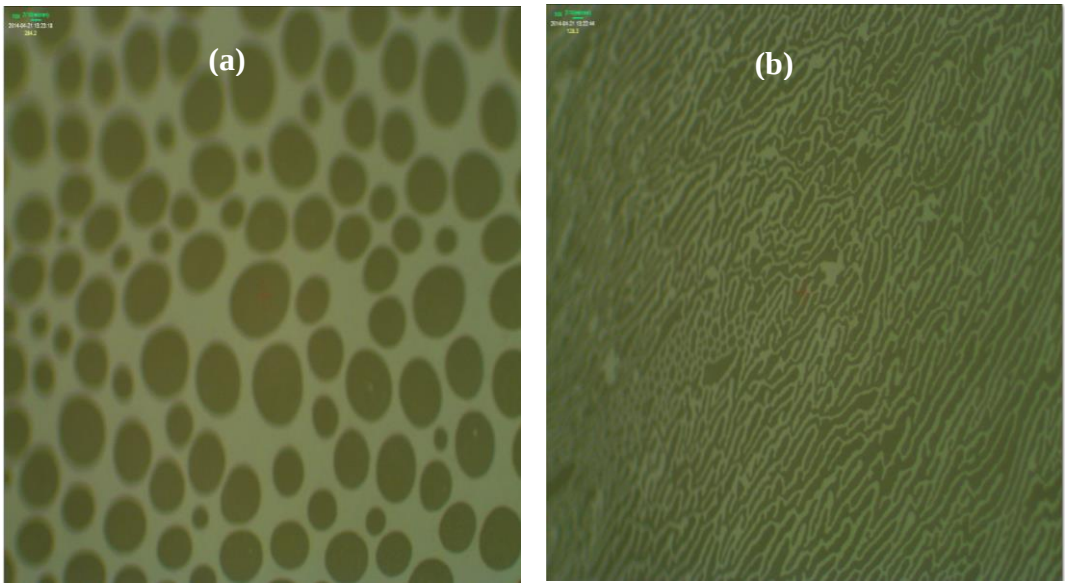

Figure 40. Nano agglomerates at ×100 magnification (a) before exposure to the magnetic field; (b) during the exposure to the magnetic field.

The Fe_3O_4 nano-modified water-based acrylic coating was applied on a mild steel disc measuring 2 cm in diameter and 1 mm thick. The coated samples were left to cure while exposed to a magnetic field with a magnetic flux density of about 10 mT, as shown in Figure 41**.** Another sample was left to cure on the mild steel disc without being exposed to the magnetic flux. After drying, they were tested using the EIS technique and impedance spectra were collected over 48 hours. Figure 42 and Figure 43 show the Nyquist and Bode plots for both samples compiled. The impedance and Nyquist plots below show that the sample that was exposed to the magnetic field demonstrated lower performance compared to the sample that was not exposed. This can be attributed to the fact that the flux density was too strong, which pulled the particles away from the center of the disc where it was exposed to the 0.5 Molar NaCl solution.

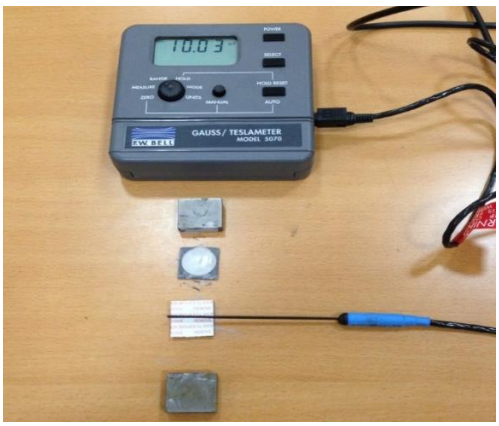

Figure 41. Coated sample between 2 permanent magnets producing a flux density of 10 mT

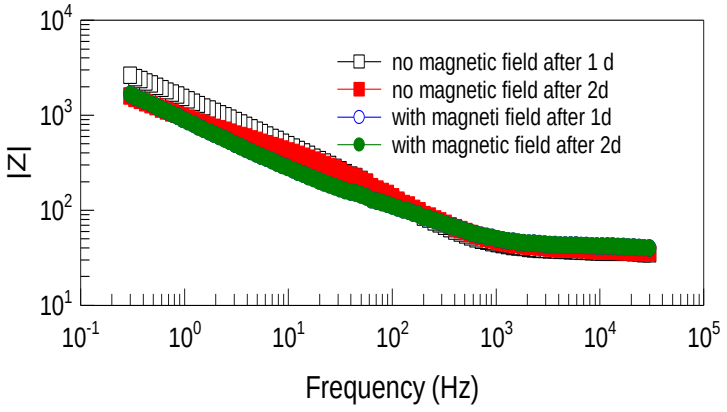

Figure 42. Impedance plot of nano- modified water-based acrylic coating showing effect of magnetic field

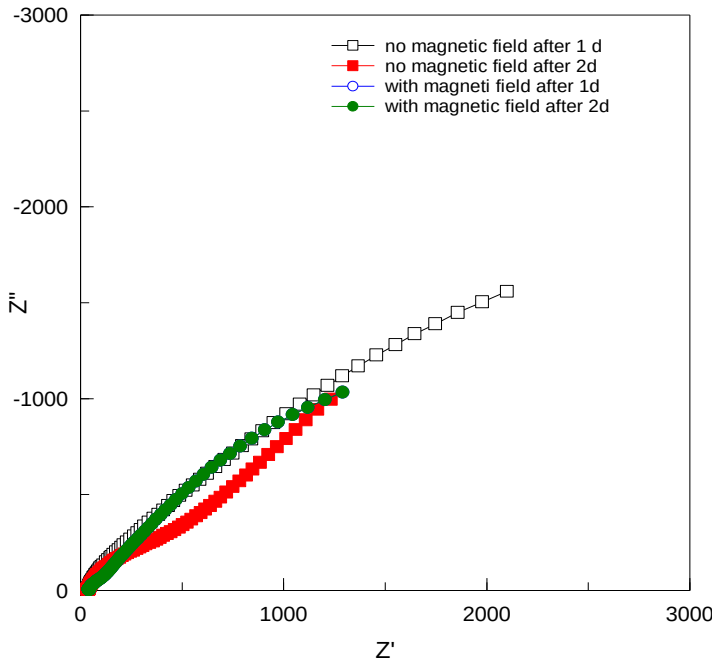

Figure 43. Nyquist plot of nano- modified water-based acrylic coating showing effect of magnetic field

Chapter 5: Conclusion

The study showed that fig leaves extract works as a corrosion inhibitor for protecting bare mild steel in 0.5M NaCl solution, and perhaps as a corrosion-inhibiting additive to water-based coatings. The use of fig leaves extract decreased the corrosion rate of bare mild steel in 0.5M NaCl solution and resulted in average inhibition efficiency over the test period of 69%. The reduction in the corrosion rate can be attributed to the adsorption of the inhibitor molecules onto the metal surface and the formation of a protective barrier of one or several molecular layers. This protective molecular layer is believed to replace water molecules and decrease the diffusion rate of the reactant elements into the metal surface. It is also believed that this layer changes and suppresses the kinetics of cathodic and anodic reactions. It is also worth mentioning that the inhibition effect of the extract appeared to be stable over the three-week period. The study has also shown that adjusting the pH value from 5.2 to 7 increased the average corrosion inhibition efficiency over the 21 days from 69% to 82%. The fig leaves extract was also incorporated into a water-based acrylic coating during the grinding phase. This addition increased the average R_{po} values of the coating over the test period from 5041 $\Omega.cm^2$ to 8773 $\Omega.cm^2$. It also showed lower values for C_c compared to the control coating, indicating that fig leaves extract may have a corrosion-inhibitive effect. The inhibitive effects of the fig leaves extract are believed to provide corrosion protection by decreasing the activity of both anodic and cathodic reactions by releasing passivating ions.

The effect of Fe_3O_4 nano-particles on the corrosion protection properties of an alkyd-based enamel coating was investigated. It was found that the addition of 1% wt. of nano- Fe_3O_4 particles might improve the corrosion resistance and adhesion of alkyd-based enamel coatings, provided that a proper distribution of nano-particles is achieved. The impact of incorporating 1% wt. nano-Fe_3O_4 particles resulted in an increase in the impedance modulus at the low-frequency limit $|Z|_{0.3\ Hz}$ from an average value of 2.44E+8 $\Omega.cm^2$ to 9.00E+8 $\Omega.cm^2$. The maximum phase angle at the high frequency limit also showed higher values than the control enamel coating, indicating a better performance. This was also to be concluded by comparing the water uptake and C_c values of both coatings. Introducing the use of glass beads during the grinding phase resulted in enhancing the performance of the nano-modified coating. This coating showed lower impedance modulus $|Z|_{0.3\ Hz}$ after one day and two days. However, this

trend was reversed after seven days of immersion, showing 153% and 96% higher $|Z|_{0.3\ Hz}$ values than the control and nano-modified coatings. At 21 days, the impact was even more dominant, showing 483% and 275% higher $|Z|_{0.3\ Hz}$ values than the control and nano-modified coating, respectively. This was also confirmed by the sudden change in the rate of change in R_{cor} values at the seventh day. The use of glass beads during the grinding phase of the coating resulted in an increase in R_{cor}, after 21 days, which is 2373% and 6832% higher than the control and nano-modified coatings, respectively. It also led to lower water uptake values during the 21-day immersion period, an average of 35% reduction in the water uptake compared to the other two coatings. This might be linked to achieving better distribution of the nano-particles throughout the coating matrix. Nevertheless, optimizing the loading percentage and improving the dispersion of nano-Fe_3O_4 using other grinding mediums can further improve the performance properties of the coating.

The incorporation of Fe_3O_4 nano-particles into the water-based coating required preparing an aqueous dispersion of the particles. However, the very weak protective properties of the formulated water-based acrylic coating made the EIS technique insensitive to the changes in the coating system due to the degradation process. Therefore, it was difficult to infer the impact of the nano-particles on the water-based coating.

Finally, an attempt to investigate the effect of exposing the Fe_3O_4 nano-modified coating to a magnetic field on its protective properties was made. No clear effect on the performance was observed. This can be attributed to the weak coating matrix in which the particles were impregnated and the lack of ability to determine the flux density required to achieve suspension of the particles rather than a pulling effect from the matrix.

References

[1] P. A. Sørensen, S. Kiil, K. Dam-Johansen and C. E. Weinell, "Anticorrosive Coatings: a Review," *Journal of Coatings Technology and Research,* vol. 6, no. 2, pp. 135-176, 2009.

[2] M. Behzadnasab, S.M. Mirabedini, K. Kabiri and S. Jamali, "Corrosion Performance of Epoxy Coatings Containing Silane Treated ZrO2 nanoparticles on Mild Steel in 3.5% NaCl Solution," *Corrosion Science,* vol. 53, no. 1, pp. 89-98, 2011.

[3] S. K. Dhoke, A.S. Khanna and T. Jai Mangal Sinha, "Effect of Nano-ZnO Particles on the Corrosion behaviour of Alkyd-Based Waterborne Coatings," *Progress in Organic Coatings,* vol. 64, no. 4, pp. 371-382, 2009.

[4] A.S. Khanna and S. K. Dhoke, "Electrochemical Impedance Spectroscopy (EIS) Study of Nano-Alumina Modified Alkyd based waterborne Coatings," *Progress in Organic Coatings,* vol. 74, no. 1, pp. 92-99, 2012.

[5] P. R. Roberge, *Handbook of Corrosion Engineering*, New York: McGraw-Hill, 2000.

[6] Amy Forsgren, *Corrosion Control Through Organic Coatings*, New York: Taylor and Francis group, LLC, 2006.

[7] D. Talbot and J. Talbot, *Corrosion Science and Technology*, Boca Raton: CRC Press LLC, 1998.

[8] T. Ibrahim and M. Habbab, "Corrosion Inhibitation of Mild Steel in 2M HCI Using Aqueous Extract of Eggplant Peel," *Electrochemical Science,* vol. 6, pp. 5357-5371, 2011.

[9] Sébastien Touzain, "Some Comments on the Use of the EIS Phase Angle to Evaluate Organic Coating Degradation," *Electrochimica Acta,* vol. 55, no. 21, pp. 6190-6194, 2010.

[10] P. B. Raja and M. G. Sethuraman, "Natural products as corrosion inhibitor for metals in corrosive media — A review," *Materials letter,* vol. 62, no. 1, pp. 113-116, 2008.

[11] A.Mathiazhagan and R. Joseph, "Nanotechnology-A New Prospective in Organic Coating - Reveiw," *International Journal of Chemical Engineering and Applications,* vol. 2, no. 4, pp. 225-237, 2011.

[12] O. Lewis, G. Critchlow, G. Wolcox, A. deeZeeuw and J. Sander, "A Study of the Corrosion Resistance of a Waterborne Acrylic Coating Modified with Nano-sized Titanium Dioxide," *Progress in Organic Coatings,* vol. 73, no. 1, pp. 88-94, 2012.

[13] M. Sabzi, S. M. Mirabedini, J. Zohuriaan-Mehr and M. Atai, "Surface modification of TiO2 nano-particles with silane coupling agent and investigation of its effect onthe properties of polyurethane composite coating," *Progress in Organic Coatings,* vol. 65, no. 2, p. 222–228, 2009.

[14] A. Kalendova, "Effects of particle sizes and shapes of zinc metal on the properties of anticorrosive coatings," *Progress in Organic Coatings,* vol. 46, no. 4, p. 324–332, 2003.

[15] P. A. Schweitzer, *Paint and Coatings: Applications and Corrosion Resistance*, Boca Raton: CRC Press, 2006.

[16] D. G. Weldon, *Failure Analysis of Paints and Coatings,* Revised Edition, John Wiley & Sons, 2009.

[17] N. T. Bortak, "*Guide to Protective Coatings,Inspection and Maintenance*," United States Department of the Interior, Bureau of Reclamation, Technical Service Center, Denver, Colorado, 2002.

[18] U. Rammelt and G. Reinhard, "Characterization of Active Pigments in Damage of Organic Coatings on Steel by means of electrochemical impedance spectroscopy," *Progress in Organic Coatings,* vol. 24, no. 1-4, p. 309, 1994.

[19] T. Prosek and D. Thierry, "A Model for the Release of Chromate from Organic Coatings," *Progress in Organic Coatings,* vol. 49, no. 3, pp. 209-217, 2004.

[20] C. Hare, M. Steele and S. Collins, "Zinc Loadings, Cathodic Protection, and Post-Cathodic Protective Mechanisms in Organic Zinc-Rich Metal Primers," *Journal of Protective Coatings & Linings,* vol. 18, no. 9, pp. 54-72, 2001.

[21] R. W. Revie, *Uhlig's Corrosion Handbook,* John Wiley & Sons, 2011.

[22] S. Paul, *Surface Coatings: Science & Technology,* Chichester: John Wiley & Sons, 1996.

[23] G. W. Walter, "The application of impedance methods to study the effects of water uptake and chloride ion concentration on the degradation of paint films—I. Attached films," *Corrosion Science,* vol. 32, no. 10, pp. 1085-1103, 1991.

[24] F. L. LaQue, *Marine Corrosion: Causes and Preventioin,* New York: John Wiley & Sons Inc, 1975.

[25] E. Potvin, L. Brossard and G. Larochelle, "Corrosion protective performances of commercial low-VOC epoxy/urethane coatings on hot-rolled 1010 mild steel," *Progress in Organic Coatings,* vol. 31, no. 4, p. 363–373, 1997.

[26] B. E. Amitha Rani and B. B. J. Basu, "Green Inhibitors for Corrosion Protection of Metals and Alloys: An Overview," *International Journal of Corrosion,* vol. 102, 2012.

[27] F. Zucchi and I. H. Omar, "Plant extracts as corrosion inhibitors of mild steel in HCl solutions," *Surface Technology,* vol. 24, no. 4, p. 391–399, 1985.

[28] E. Khamis and N. Alandis, "Herbs as New Type of Green Inhibitors For Acidic Corrosion of Steel," *Materialwissenschaft und Werkstofftechnik,* vol. 33, no. 9, p. 550–554, 2002.

[29] A. Aglan, A. Allie, A. Ludwick and l. Koons, "Formulation and evaluation of Nano-Structured Polymeric Coatings for Corrosion Protection," *Surface & Coatings Technology,* vol. 202, no. 2, pp. 370-378, 2007.

[30] X. Shi, T. A. Nguyen, Z. Suo, Y. Liu and R. Avci, "Effect of nanoparticles on the anticorrosion and mechanical properties of epoxy coating," *Surface and Coatings Technology,* vol. 204, no. 3, pp. 237-245, 2009.

[31] X. Gao, Y. Zhu, S. Zhou, W. Gao, Z. Wang and B. Zhou, "Preparation and characterization of well-dispersed waterborne polyurethane/CaCO3 nanocomposites," *Colloids and Surfaces A: Physicochemical and Engineering Aspects,* vol. 377, no. 1-3, pp. 312-317, 2011.

[32] S. K. Dhoke and A.S. Khanna, "Effect of Nano-Fe2O3 Particles on the Corrosion behaviour of Alkyd based waterborne Coatings," *Corrosion science,* vol. 51, no. 1, pp. 6-20, 2009.

[33] F.F. Xia, C. Liu, F. Wang, M.H. Wu, J.D. Wang, H.L. Fu and J.X. Wang, "Preparation and Charaterization of Nano Ni-TiN Coatings deposited by Ultrasonic Electrodeposition," *Alloys and Compounds,* vol. 490, no. 1-2, pp. 431-435, 2012.

[34] D. Loveday, P. Peterson and B. Rodgers, "Evaluation of Organic Coatings with Electrochemical Impedance Spectroscopy-Part 1: Fundamentals of Electrochemical Impedance Spectroscopy," *JCT Coatings Tech,* vol. 1, no. 8, pp. 46-52, 2004.

[35] E. barsoulov and J. R. Mcdonald, *Impedance Soectroscopy theory, Experiment, and Applications,* New jersey: John Wiley & Sons, 2005.

[36] I. A. Kartsonakis, A. C. Balaskas and G. C. Kordas, "Influence of Cerium Molydbate Containers on the Corrosion Performance of Epoxy Coated Aluminium Alloys 2024-T3," *Corrosion Science,* vol. 53, no. 11, pp. 3771-3779, 2011.

[37] T. Ibrahim and M. Abou Zour, "Corrosion Inhibition of Mild Steel Using Fig Leaves Extract in Hydrochloric Acid Solution," *Electrochemical Science,* vol. 6, pp. 6442-6455, 2011.

[38] A. M. Abdel-Gaber, B. A. Abd-El Nabey, E. Khamis, O. A. Abdelattef, H. Aglan and A. Ludwick, "Influence of natural inhibitor, pigment and extender on corrosion of polymer coated steel," *Progress in Organic Coatings,* vol. 69, no. 4, pp. 402-409, 2010.

[39] A. Monshi, M. R. Foroughi and M. R. Monshi, "Modified Scherrer Equation to Estimate More Accurately Nano-Crystallite Size Using XRD," *World Journal of Nano Science and Engineering,* vol. 2, pp. 154-160, 2012.

[40] M. Bethencourt, F. J. Botana, M. J. Cano, R. M. Osuna and M. Marcos, "Lifetime prediction of waterborne acrylic paints with the AC–DC–AC method," *Progress in Organic Coatings,* vol. 49, no. 3, pp. 275-281, 2004.

[41] Y. Zhu, J. Xiong, T. Yuming and Y. Zuo, "EIS study on failure process of two polyurethane composite coatings," *Progress in Organic Coatings,* vol. 69, no. 1, pp. 7-11, 2010.

[42] Z. Sharer and J. Sykes, "Insights into protection mechanisms of organic coatings from thermal testing with EIS," *Progress in Organic Coatings,* vol. 74, no. 2, pp. 405-409, 2012.

[43] X. Liu, J. Xiong, Y. Lv and Y. Zuo, "Study on corrosion electrochemical behavior of several different coating systems by EIS," *Progress in Organic Coatings,* vol. 64, no. 4, p. 497–503, 2009.

[44] D.J. Mills, S.S. Jamali and K. Paprocka, "Investigation into the effect of nano-silica on the protective properties of polyurethane coatings," *Surface and Coatings Technology,* vol. 209, p. 137–142, 2012.

[45] J. M. McIntyre and H. Q. Pham, "Electrochemical impedance spectroscopy; a tool for organic coatings optimizations," *Progress in Organic Coatings,* vol. 21, no. 1-4, pp. 201-207, 196.

[46] S. Taylor and C. hunter, "Predicting the Long Term Performance of Coatings from Short Term EIS data," *ECS transactions,* vol. 13, no. 13, pp. 43-53, 2009.

[47] S. Taylor, F. Contu, L. Calle, J. Curran and W. Li, "Predicting the long term Field performance of coating Systems on Steel using a Rapid Electrochemical test: The Damage Tolerance Test," *Corrosion Science,* vol. 68, no. 3, 2012.

[48] G. Grundmeier, W. Schmidt and M. Stratmann, "Corrosion Protection by Organic Coatings: Electrochemical Mechanism and Novel Methods of Investigation," *Electrochimica Acta,* no. 45, pp. 2515-2533, 2000.

[49] A. Groysman, *Corrosion for Everybody,* London: Springer, 2010.

[50] S. Garcia and J.Suay, "Optimization of Deposition Voltage of Cataphoretic Automotive Primers Assessed by EIS and AC/DC/AC," *Organic Coatings,* no. 66, pp. 306-313, 2009.

[51] L. Fenzy, "An Electrochemical Method for the Quantification and Prediction of the Long Term Performance of Coated AA2024-T3," *M.S. Thesis University of verginia,* 2006.

[52] F. Contu, S. Taylor, L. Calle, P. Hintze, J. Curran and W. Li, "The Prediction of Long Term Coating Performance from Short Term Elechtrochemical Data, Part II. Comparison of Electrochemical Data to Field Exposure Results for Coatings on Steel," *Organic Coatings,* vol. 24, no. 1, pp. 197-209, 2010.

[53] L. L. Vatta, R. D. Sanderson and K. R. Koch, "Magnetic nanoparticles: Properties and potential applications," *Pure Appl. Chem.,* vol. 78, no. 9, p. 1793–1801, 2006.

[54] A.Y. El-Etre and M. Abdallah, "Natural honey as corrosion inhibitor for metals and alloys. II. C-steel in high saline water," *Corrosion Science,* vol. 42, no. 4, p. 731–738, 2000.

[55] A. Y. El-Etre, "Khillah extract as inhibitor for acid corrosion of SX 316 stee," *Applied Surface Science,* vol. 252, no. 24, p. 8521–8525, 2006.

[56] [Online]. Available: http://www.eiscourse.com/. [Accessed 3 January 2014].

[57] M. Stratmann, H. Streckel, K. T. Kim and S. Crockett, "On the atmospheric corrosion of metals which are covered with thin electrolyte layers-iii. the measurement of polarisation curves on metal surfaces which are covered by thin electrolyte layers," *Corrosion Science,* vol. 30, no. 6-7, pp. 715-734, 1990.

[58] A. Forsgren and D. Thierry, *"Corrosion properties of coil-coated galvanized steel,using field exposure and advanced electrochemical techniques,"* Swedish Corrosion Institute (SCI), Stockholm, 2001.

[59] A. J. Bard and L. R. Faulkner, *Electrochemical Methods: Fundamentals and Applications,* New York: John Wiley & Sons, 2001.

[60] A. G. Gilicinsk and C. R. Hegedus, "New applications in studies of waterborne coatings by atomic force microscopy," *Progress in Organic Coatings,* vol. 32, no. 1-4, pp. 81-88, 1997.

[61] E. Almeida, M. Balmayore and T. Santos, "Some relevant aspects of the use of FTIR associated techniques in the study of surfaces and coatings," *Progress in Organic Coatings,* vol. 44, no. 3, pp. 233-242, 2002.

[62] B. S. Skerry and D. A. Eden, "Characterisation of coatings performance using electrochemical noise analysis," *Progress in Organic Coatings,,* vol. 19, no. 4, pp. 379-396, 1991.

[63] A. El-Hosary, M. Gowish and R. Saleh, " 2nd International Symposium and Oriented Basic Electrochemistry," in *Evaluation of quinolines as inhibitors* , Madras, 1980.

[64] A. Y. El-Etri, M. Abdallah and Z. E. El-Tantawy, "Corrosion inhibition of some metals using lawsonia extract," *Corrosion Science,* vol. 2, no. 47, p. 385–395, 2005.

[65] K. Pravinar, A. Hussein, G. Varkey and G. Singh, "Inhibition effect of aqueous extracts of Eucalyptus leaves on the acid corrosion of mild steel and copper," *Transaction of the SAEST,* vol. 28, no. 1, p. 8–12, 1997.

[66] S. A. Verma and G. N. Mehta, "Effects of acid extracts of powered seeds of Eugenia Jambolans on corrosion of mild steel in HCl-study by DC polarisation techniques," *Transaction of the SAEST,* vol. 32, no. 4, p. 89–93, 1997.

[67] S. J. Zakvi and G. N. Mehta, "Acid Corrosion of Mild Steel and Its Inhibition by Swertia Aungustifolia-Study by Electrochemical Techniques," *Transaction of the SAEST,* vol. 23, pp. 407-412, 1988.

[68] P. Sakthivel, P. V. Nirmala, S. Umamaheswari, A. Arul Antony, G. P. Kalignan, A. Gopalan and T. Vasudevan, "Corrosion inhibition of mild steel by extracts of Pongamia Glabra and Annona Squamosa in acidic media," *Bulletin of Electrochemistry,* vol. 15, no. 2, p. 83–86, 1999.

[69] E. E. Ebenso and U. J. Ekpe, "Kinetic study of corrosion and corrosion inhibition of mild steel in H2SO4 using Carica papaya leaves extract," *West African Journal of Biological and Applied Chemistry,* vol. 41, pp. 21-27, 1996.

[70] C. A. Loto, "The Effect of Bitterleaf Extracts on Corrosion of Mild Steel in 0.5M HCl and H2SO4 Solutions," *Nigeria Corrosion Journal International,* vol. 1, pp. 19-20, 1998.

[71] A. Chetouani and B. Hammouti, "Corrosion inhibition of iron in hydrochloric acid solutions by naturally henna," *Bulletin of Electrochemistry,* vol. 19, no. 1, p. 23–25, 2003.

[72] A. Bouyanzer and B. Hammouti, "Naturally occurring ginger as a corrosion inhibitor for steel in molar hydrochloric acid at 353 K," *Bulletin of Electrochemistry,* vol. 20, no. 2, pp. 63-65, 2004.

[73] A. Bouyanzer and B. Hammouti, "A study of anti-corrosive effects of Artemisia oil on steel," *Pigment & Resin Technology,* vol. 33, no. 5, pp. 287-292, 2004.

[74] A. Chetouani , B. Hammouti and M. benkaddour, "Corrosion inhibition of iron in hydrochloric acid solution by jojoba oil," *Pigm. Resin Technology,* vol. 33, no. 1, pp. 26-31, 2004.

[75] E. E. Oguzie, "Inhibition of acid corrosion of mild steel by Telfaria occidentalis extract," *Pigment and Resin Technology,* vol. 34, no. 6, pp. 321-326, 2005.

[76] Yan Li, Peng Zhao, Qiang Liang and Baorong Hou, "Berberine as a natural source inhibitor for mild steel in 1M H2SO4," *Applied Surface Science,* vol. 252, no. 5, pp. 1245-1253, 2005.

[77] B.R. Hinderliter, S.G. Croll, D.E. Tallman, Q. Su and G.P. Bierwagen, "Interpretation of EIS Data from Accelerated Exposure of Coated Metals Based on Modeling of Coating Physical Properties," *Electrochimica Acta,* vol. 51, no. 21, pp. 4505-4515, 2006.

[78] R.G. Duarte, A.S. Castela and M.G.S. Ferreira, "A new model for estimation of water uptake of an organic coating by EIS: The tortuosity pore model," *Progress in Organic Coatings,* vol. 65, no. 2, pp. 197-205, 2009.

[79] A.S. Castela and A.M. Simões, "An impedance model for the estimation of water absorption in organic coatings. Part I: A linear dielectric mixture equation," *Corrosion Science,* vol. 45, no. 8, p. 1631–1646, 2003.

[80] A. A. El Hosary, R. M. Saleh and A. M. Shams El Din, "Corrosion inhibition by naturally occurringsubstances-I. The effect of Hibiscus subdariffa (karkade) extract on the dissolution of Al and Zn," *Corrosion Science,* vol. 12, no. 12, p. 897–904, 1972.

[81] Shik Chi Tsang, Valérie Caps, Ioannis Paraskevas, David Chadwick and David Thompsett, "Magnetically Separable, Carbon-Supported Nanocatalysts for the Manufacture of Fine Chemicals," *Angewandte Chemie,* vol. 116, no. 42, p. 5763–5767, 2004.

[82] R. A. L. Sathiyanathan, S. Maruthamuthu and M. Selvanayagam, "Corrosion inhibition of mild steel by ethanolic extracts of Ricinus communis leaves," *Indian Journal of Chemical Technology,* vol. 12, no. 3, pp. 356-360, 2005.

[83] S. Chikazumi, S. Taketomi, M. Ukita, M. Mizukami, H. Miyajima, M. Setogawa and Y. Kurihara, "Physics of magnetic fluids," *Journal of Magnetism and Magnetic Materials* , vol. 65, pp. 245-251, 1987.

[84] D. W. Elliot and W. Zhang, "Field assessment of nanoscale bimetallic particles for groundwater treatment," *Environmental Science and Technology,* vol. 35, pp. 4922-4926, 2001.

[85] J. R. Davis, *Corrosion: Understanding the Basics,* ASM International, 2000.

[86] J. Bordziłowski, A. Królikowska, P.L. Bonora, I. Maconi and A. Sollich, "Underwater EIS measurements," *Progress in Organic Coatings,* vol. 67, no. 4, pp. 414-419, 2010.

[87] Abdel Salam Hamdy, A.G. Sa'eh, M.A. Shoeib and Y. Barakat, "Evaluation of Corrosion and Erosion-Corrosion resistance of Mild Steel in Sulfide-Containing NaCl Aerated Solutions," *Electrochimica Acta,* vol. 52, no. 24, pp. 7068-7074, 2007.

[88] S. Afroukhteh, C. Dehghanian and M. Emamy, "Preparation of the Ni-P Composite Coating Co-Deposited by Nano TiC particles and Evaluation of its Corrosion Property," *Applied Surface Science,* no. 258, pp. 2597-2601, 2012.

[89] M. Takafuji, S. Ide, H. Ihara and Z. Xu, "Preparation of Poly(1-vinylimidazole)-Grafted Magnetic Nanoparticles and Their Application for Removal of Metal Ions," *Chemistry of Materials,* vol. 16, no. 10, pp. 1977-1983, 2004.

[90] K. S. Parikh and K. J. Joshi, "Natural compounds onion (Allium cepa), garlic (Allium sativum) and bitter gourd (Momordica charantia) as corrosion inhibitors for mild steel in hydrochloric acid," *Trans. SAEST.,* vol. 39, no. 1-2, pp. 29-35, 2004.

[91] R. G. Kelly, J. R. Scully, D. W. Shoesmith and R. G. Buchheit, Electrochemical Techniques in Corrosion Science and Engineering, New York: Marcel Dekker, Inc., 2003.

[92] M. Orazem and B. Tribollet, *Electrochemical Impdedance Spectroscopy,* New Jersey: John Wiley & Sons, 2008.

[93] R. M. Saleh, A. A. Ismall and A. A. El Hosary, "Corrosion Inhibition by Naturally Occurring Substances: VII. The effect of aqueous extracts of some

leaves and fruit-peels on the corrosion of steel, Al, Zn and Cu in acids," *British Corrosion,* vol. 17, no. 3, p. 131–135, 1982.

[94] M. J. Sanghvi, S. K. Shukla, A. N. Misra, M. R. Padh and G. N. Mehta, "Inhibition of hydrochloric acid corrosion of mild steel by acid extracts of Embilica officianalis, Terminalia bellirica and Terminalia chebula," *Bulletin of Electrochemistry,* vol. 13, no. 8-9, p. 358–361, 1997.

[95] M. J. Sanghvi, S. K. Shukla, A. N. Misra, M. R. Padh and G. N. Mehta, "Corrosion inhibition of mild steel in hydrochloric acid by acid extracts of Sapindus trifolianus, Acacia Concian and Trifla," *Transactions of the Metal Finishers Association of India,* vol. 5, no. 3, p. 143–147, 1996.

[96] U. J. Ekpe, E. E. Ebenso and U. J. Ibok, "Inhibitory action of Azadirachta indica leaves extract on the corrosion of mild steel in H2SO4," *West African Journal of Biological and Applied Chemistry,* vol. 37, p. 13–30, 1994.

[97] T. Ibrahim, Y. Chehade and M. Abou Zour, "Corrosion Inhibition of Mild Steel using Potato Peel Extract in 2M HCl Solution," *Int. J. Electrochem. Sci,* vol. 6, pp. 6542 - 6556, 2011.

[98] T. Ibrahim, H. Alayan and Y. Al Mowaqet, "The Effect of thyme leaves Extract on Corrosion of Mild Steel in HCI," *Progress in Organic Coatings,* vol. 75, no. 4, pp. 456-462, 2012.

[99] H. Vaghari, Z. Sadeghian and M. Shahmiri, "Investigation on Synthesis, Characterisation and Electrochemical Properties of TiO2-Al2O3 Nanocomposite Thin Film Coated on 316L Stainless Steel," *Surface & Coatings Technology,* vol. 205, no. 23-24, pp. 5414-5421, 2011.

[100] N. Selvakumar, K. Jeyasubramanian and R. Sharmila, "Smart Coating for Corrosion Protection by Adopting Nano Particles," *Progress in Organic Coatings,* vol. 74, no. 3, pp. 461-469, 2012.

[101] V. Chawla, D. Puria, S. Prakash, A. Chawla and B. S. Sidhu, "Characterization and Comparison of Corrosion Behaviour of Nanostructured TiAlN and AlCrN Coatings on Superfer 800H (INCOLOY 800H) Substrate," *Journal of Minerals & Materials Characterization & Engineering,* vol. 8, no. 9, pp. 715-727, 2009.

[102] A.-H. Lu, E. L. Salabas and F. Schüth, "Magnetic Nanoparticles: Synthesis, Protection, Functionalization, and Application," *Angewandte Chemie International Edition,* vol. 46, no. 8, pp. 1222-1244, 2007.

[103] S. R. Taylor, F. Contu, C. Hunter and L. fenzy, "The Prediction of Long Term Coatings Performance from Short Term Elechtrochemical Data, Part I. Inhibited Aerospace Coating Systems-Comparison to Salt Spray Data," *Organic Coatings,* vol. 24, no. 1, pp. 185-196, 2010.

[104] M. Kendig, S. Jeanjaquet, R. Brown and F. Thomas, "Rapid Electrochemical Assessment to Paint (REAP)," *Journal of Coatings Technology,* vol. 68, no. 863, p. 39, 1996.

[105] A. H. Lu, W. Schmidt, N. Matoussevitch, H. Bonnermann, B. Spliethoff, B. Tesche, E. Bill, W. Kiefer and F. Schuth, "Nanoengineering of a Magnetically Separable Hydrogenation Catalyst," *Angewandte Chemie International Edition,* vol. 43, no. 33, p. 4303–4306, 2004.

[106] D. Loveday, P. Peterson and B. Rodgers, "Evaluation of Organic Coatings with Electrochemical Impedance Spectroscopy-Part 2: Application of EIS to Coatings," *JCT coatingstech,* vol. 1, no. 10, pp. 88-93, 2004.

[107] B. Hammouti, S. Kertit and M. Mellhaoui, "Bgugaine: a natural pyrollidine alkaloid product as corrosion inhibitor of iron in HCl medium," *Bulletin of Electrochemistry,* vol. 11, no. 12, p. 553, 1995.

Vita

Khalil Abed received his B.Sc. degree in Industrial Engineering from Jordan University of Science and Technology in 2005. Mr. Abed received a certificate of appreciation from Jordan University and Technology, under the patronage of His Royal Highness Prince Faisal Bin Al-Hussain, for his outstanding academic achievements for the year 2001. During his student time at the university, he was an active member of the society and received several awards and certificates of appreciation from several local and international youth organizations.

Mr. Abed held several technical and managerial positions at renowned multinational companies in both construction and oil and gas sectors. He started his career in 2005 as a field engineer at Hilti Jordan. In 2010, Mr. Abed joined Tyrolit Middle East FZE as a Product Manager for construction and industrial products. At present, he is the Business Development Manager for Kingdom of Suadi Arabia, North Africa and Levant markets at Cortec Middle East FZC.

Mr. Abed has coauthored and published a technical paper entitled “The effect of time and temperature on the precipitation behavior and hardness of Al–4 wt%Cu alloy using design of experiments” Journal of Materials Processing Technology, vol. 204, no. 1-3, pp. 343-349, 2008.